MIXED MATRIX MEMBRANE FOR CO_2 SEPARATION FROM NATURAL GAS

BY

Abdelrahman Mohammedelfatih Awad Babiker

A Thesis Presented to the

DEANSHIP OF GRADUATE STUDIES

KING FAHD UNIVERSITY OF PETROLEUM & MINERALS

DHAHRAN, SAUDI ARABIA

In Partial Fulfillment of the

Requirements for the Degree of

MASTER OF SCIENCE

In

CHEMICAL ENGINEERING

May 2017

KING FAHD UNIVERSITY OF PETROLEUM & MINERALS

DHAHRAN- 31261, SAUDI ARABIA

DEANSHIP OF GRADUATE STUDIES

This thesis, written by **Abdelrahman Mohammedelfatih Awad** under the direction his thesis advisor and approved by his thesis committee, has been presented and accepted by the Dean of Graduate Studies, in partial fulfillment of the requirements for the degree **MASTER OF SCIENCE IN CHEMICAL ENGINEERING.**

Dr. Isam Aljundi

(Advisor)

Dr. Mohammed Ba-Shammakh
Department Chairman

Dr. Mamdoh Al-Harthi
(Member)

Dr. Salam A. Zummo
Dean of Graduate Studies

Dr. Sulaiman Al-Khattaf
(Member)

22/5/12

Date

To my parents, brothers, and sisters

for their help, limitless support and prays

ACKNOWLEDGMENTS

All praise and glory are to **Allah** the most Merciful and Beneficent, I thank **Allah** almighty for his generosity, help, and giving me the health and power to complete this work. Peace and blessing of Allah be upon the **Holy Prophet Mohammed**, the best of mankind.

I would like to express my profound gratitude and warmest appreciation to my thesis advisor **Dr. Isam Al Jundi** for his valued guidance, countless efforts, professional advice, and critical supervision from the starting of this work until the end. Dr. Isam has not only provided me with guidance during my research activities but he has also given generously of his time to offer encouragement, advice, and support. Many thanks and appreciation also go to committee members **Dr. Mamdouh Al Harthi** and **Dr. Sulaiman Al Khattaf** for their guidance, support, and invaluable suggestions for this research. I am thankful for the time devoted by them to correct and review this work.

Never been forgotten, my parents, brothers, and sisters. I am deeply appreciative for their help, limitless support and prays to complete this work. I also would like to thank my friends and colleagues for their help and encouragement throughout this work.

I would like to acknowledge King Fahd University of petroleum and minerals and the Department of Chemical Engineering for giving me the opportunity to peruse my graduate studies.

TABLE OF CONTENTS

LIST OF TABLES

LIST OF FIGURES

LIST OF ABBREVIATIONS

PSF	:	Polysulfone
PA	:	Polyamide
PES	:	Polyethersulfone
PEA	:	Polyetheramine
CDC	:	Carbide-derived carbon
MMMs	:	Mixed matrix membranes
DMACs	:	N, N-dimethylacetamide
THF	:	Tetrahydrofuran
Etol	:	Ethanol
PDMS	:	Polydimethylsiloxane
TFC	:	Thin film composite
MWNTs	:	Multi-walled carbon nanotubes
PMMA	:	Polymethyl methacrylate
DI	:	Deionized water
IPC	:	Isophthaloyl chloride
PIP	:	Piprazine

TMC	:	Trimesoyl chloride
MPD	:	m-Phenylenediamine
TETA	:	Trimethylene tetramine
IF	:	Interfacial polymerization
NG	:	Natural gas
MOFs	:	Metal-organic frameworks
FT-IR	:	Fourier transformation infrared
XRD	:	X-ray Diffraction
TGA	:	Thermogravimetric Analysis
SEM	:	Scanning Electron Microscopy
BET	:	Brunauer–Emmett–Teller
R	:	Universal gas constant

ABSTRACT

Full Name : Abdelrahman Mohammedelfatih Awad Babiker

Thesis Title : Mixed matrix membrane for CO2 separation from natural gas

Major Field : Chemical Engineering

Date of Degree : May 2017

Recently, membrane technology has emerged as a competitive alternative process for CO_2 separation from natural gas. Nevertheless, it continues to seek new, robust, and economic membrane materials with superior separation performance in term of selectivity and productivity. In this research, new carbon nanomaterials (titanium carbide-derived carbon nanoparticles (CDCs)) were embedded into polyamide film to develop CDCs/Polyamide mixed matrix membranes by interfacial polymerization reaction of piperazine (PIP) and isophthaloyl chloride (IPC) supported on polysulfone (PSF) membrane. The fabricated membranes as well as CDCs nanoparticles were characterized by SEM, FT-IR, TGA, and XRD. The characterization results confirmed the successful incorporation of CDC nanoparticles into the rough polyamide layer. Moreover, thermal stability of polyamide thin film membranes was improved by adding CDCs nanoparticles. Gas permeation measurements of the fabricated membranes demonstrated 78.08% and 49.89% enhancement in CO_2 permeance and CO_2/CH_4 selectivity; respectively compared to neat polyamide membrane. CDC nanoparticles disrupted the polyamide matrix which resulted in higher free volume for gas to transport. Furthermore, the high surface area of CDCs offered more volume for gases to adsorb thereby improved separation performance was observed for CDCs/polyamide MMMs. The gas permeation tests of layer by layer MMMs revealed that building more than one selective layer on top of the polysulfone support resulted in higher CO_2/CH_4 selectivity while CO_2 permeance decreased. CDCs/polyamide MMMs with 10 selective layers showed the best separation performance with CO_2/CH_4 selectivity of 24.08.

Finally, the effect of CDC nanoparticle loading, operating temperature, and feed pressure on the separation performance were studied

ملخص الرسالة

الاسم الكامل:عبدالرحمن محمد الفاتح عوض بابكر

عنوان الرسالة: فصل غاز ثاني اوكسيد الكربون من الغاز الطبيعي باستخدام غشاء مختلط
التخصص: هندسة كيميائية

تاريخ الدرجة العلمية: مايو 2017

في الآونة الأخيرة، ظهرت تكنولوجيا الأغشية كعملية بديلة لمنافسه العمليات التقليديه المستخدمه في فصل غاز ثاني أكسيد الكربون من الغاز الطبيعي. بالرغم من ذالك، فإن تكنولوجيا الاغشيه لاتزال تسعى لاستخدام مواد جديدة، قوية، واقتصادية مع أداء عمليه الانفصال بصوره اكثر تفوقا في مجالي الانتقائية والإنتاجية. في هذا العمل البحثي، تم تحضير أغشية بوليسولفون واستخدامها كداعم لتصنيع الأغشية الرقيقة من مادة البولي أميد. علاوة على ذلك، تم تضمين جزيئات الكربون المستمدة من كربيد التيتانيوم في طبقه البولي أميد لتصنيع الغشاء المختلط لتطبيق فصل الغاز.تم استخدام طريقة التحويل الجاف / الرطب لتحضير الغشاء الداعم (بوليسولفون). في حين تم تصنيع غشاء البولي أميد و الغشاء المختلط من جزيئات الكربون / بولي أميد باستخدام تفاعل البلمرة.. أخذت صوربواسطه مجهر الكتروني لدراسة شكل الاغشيه (مورفولوجيا الأغشية) وأظهرت النتائج أن البوليسولفون الداعم لديه سطح أملس على نحو سلس وكان هذا السطح مغطاة تماما بطبقة البولي أميد الخام، كما أكدت الصور اللمجهريه عمليه دمج الجسيمات النانوية في طبقة البولي أميد.بالاضافه لذالك تمت دراسة التركيب الكيميائي للأغشيه باستخدام أطياف الاشعه تحت الحمراء التي أكدت وجود مجموعات وظيفية من مادة البولي أميد. وعلاوة على ذلك، كشف التحليل الحراري أن إضافة الجزيئات النانوية إلى غشاء البولي أميد عززالاستقرار الحراري للأغشية البولي أميد. تمت دراسه النفاذيه وقابليه الفصل للاغشيه باستخدام غازي ثاني اكسيد الكربون والميثان وأظهرت لنتائج أن بناء طبقة البولي أميد فوق غشاء بوليسولفون يعزز انتقائية الغشاء لغاز ثاني اكسيد الكربون.وان الاغشيه المختلطه لها نفاذيه اعلي بنسبه 78.08% مقارنه بغشاء البولي اميد من غير جزيئات الكربون. بالاضافه لذالك الاغشيه لديها ايضا قابليه اعلي للفصل بنسبه 49.89%. وأخيرا، تم دراسة تأثيرتركيزالجسيمات المتناهية الصغرفي الغشاء، درجة حرارة التشغيل، ضغط الغاز،درجه الحراره، وعدد الطبقات الانتقائية على أداء الفصل للأغشية .

CHAPTER 1

INTRODUCTION

1.1 Background on natural gas:

As the global economy rises, the demand for clean energy supply is increasing continuously. Nowadays, natural gas plays a significant strategic role in the energy supply to provide a high-quality energy source that is economically viable, and environmentally sustainable. In spite the fact that the energy content per volume in NG is lower than other fossil fuels, natural gas is more efficient in energy conversion and has higher hydrogen content [1]. In 2004, NG constituted almost 23.5% of energy source around the world right after oil (constituted 35.3%). Recently, NG accounts for $22 billion per year in the world market [2]. As the importance of natural gas is increasing, more information and knowledge on natural gas processing and purification are required using novel and robust techniques [2].

Natural gas is formed by decomposition of living organisms like plant, animal, and micro-organism which have been living over a long time ago and have become an inanimate gas mixture. Natural gas is classified as associated NG that is produced from oil wells and non-associated NG. The constitution of natural gas is mainly methane (accounts for seventy to ninety percent of the total components) and other light and heavier hydrocarbon as well as other impurities such as CO_2, N_2, Hg, He, H_2S. Actually, the composition of the gas

depends on the type of the gas and how deep is the location of the reservoirs. Table 1.1 represents the natural gas composition in different reservoirs around the world [3].

Table 1.1: The natural gas composition in different reservoirs around the world [3]**.**

	Reservoir				
Component	Groningen (Netherlands)	Laeq (France)	Uch (Pakistan)	Uthmaniyah (Saudi Arabia)	Ardjuna (Indonesia)
CH_4	81.3	69	27.3	55.5	65.7
C_2H_6	2.9	3	0.7	18	8.5
C_3H_8	0.4	0.9	0.3	9.8	14.5
C_4H_{10}	0.1	0.5	0.3	4.5	5.1
C_{5+}	0.1	0.5	-	1.6	0.8
N_2	14.3	1.5	25.2	0.2	1.3
H_2S	-	15.3	-	1.5	-
CO_2	0.9	9.3	46.2	8.9	4.1

No doubt, natural gas has a wide range of applications including petrochemical feedstocks, transportation for industry, commercial, residential usage, and electricity generation. Figure 1.1 shows the proportion of these applications for the year 2009 [3].

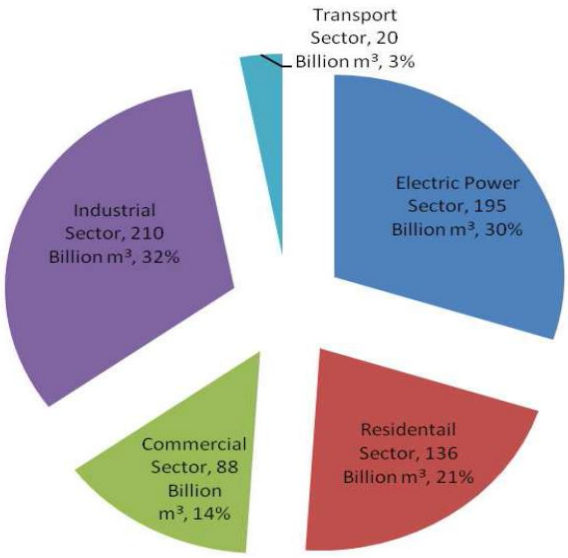

Figure 1.1: The proportion of different natural gas applications for the year 2009 [3]

1.2 Natural gas sweetening process:

In gas sweetening process impurities (such as CO_2 and H_2S) are removed from the natural gas stream in order to meet the standard quality specification set by pipeline transmission and distribution companies (see Table 1.2). Carbon dioxide in natural gas reduces the calorific value of the gas and affects the selling price. Furthermore, in presence of water, the gas stream becomes acidic and corrosive which damages pipelines and equipment [3]. Therefore, CO_2 removal from natural gas has the synergistic effects of controlling the greenhouse gas emissions (GHE) and economical beneficial of lower transportation cost through possibilities of gas compression and volume reduction [2]. On the other hand, CO_2 separation could produce a highly concentrated CO_2 stream that can be used in enhanced oil recovery (EOR) after its removal from natural gas stream and in other chemical industries rather than direct release into the atmosphere [2]. Therefore, CO_2/CH_4 separation using economical and more effective techniques as well as CO_2 capture at a wide range of

concentration are attracting a great deal of interest in chemical engineering processes [1]. However, CO_2 capture from natural gas using more efficient and robust technique is still one of the challenges in gas separation application [3].

Table 1.2: Natural gas specifications for commercial applications [4].

Component	Typical Feed	Sales Specifications
CH_4	70 - 80%	90%
CO_2	5 - 20%	< 2%
C_2H_6	3 - 4%	3 - 4%
C3 to C5	~ 3%	~ 3%
N_2	~ 1 - 4%	< 4%
H_2S	< 100 ppm	< 4 ppm
H_2O	Saturated	< 100 ppm
C6 and higher	0.5 - 1%	0.5 - 1%

Owing to the abundance of CO_2 in raw NG, it has attracted more research attention than H_2S [4]. CO_2 removal from natural gas is commonly achieved using absorption, adsorption, cryogenic or condensation, or membrane process [2]. Each of these processes has its own advantages and drawbacks. Among which, amine absorption process is the most developed commercial technology. Figure 1.2 shows the common technologies for natural gas purification.In absorption process, gasses are placed in contact with a soluble liquid. This process can be classified as: (1) physical absorption which is achieved based on the gasses solubilities and mass transfer rates, and (2) chemical absorption that is based on the reaction equilibria and kinetics. The drawback of this process is that the solvent for the absorption in a process like amines leads to corrosion problem. The reaction between the solvent and some corrosion inhibitors causes erosion problem, high foaming tendency, and solid suspension which reduce the loading of CO_2 gas and solvent. So, antifoaming agent injection is required for surface tension reduction of the solvent in order to enhance

CO_2/solvent contact. Moreover, all solvent cannot be recycled to the column which causes environmental hazards from the solvent disposal.

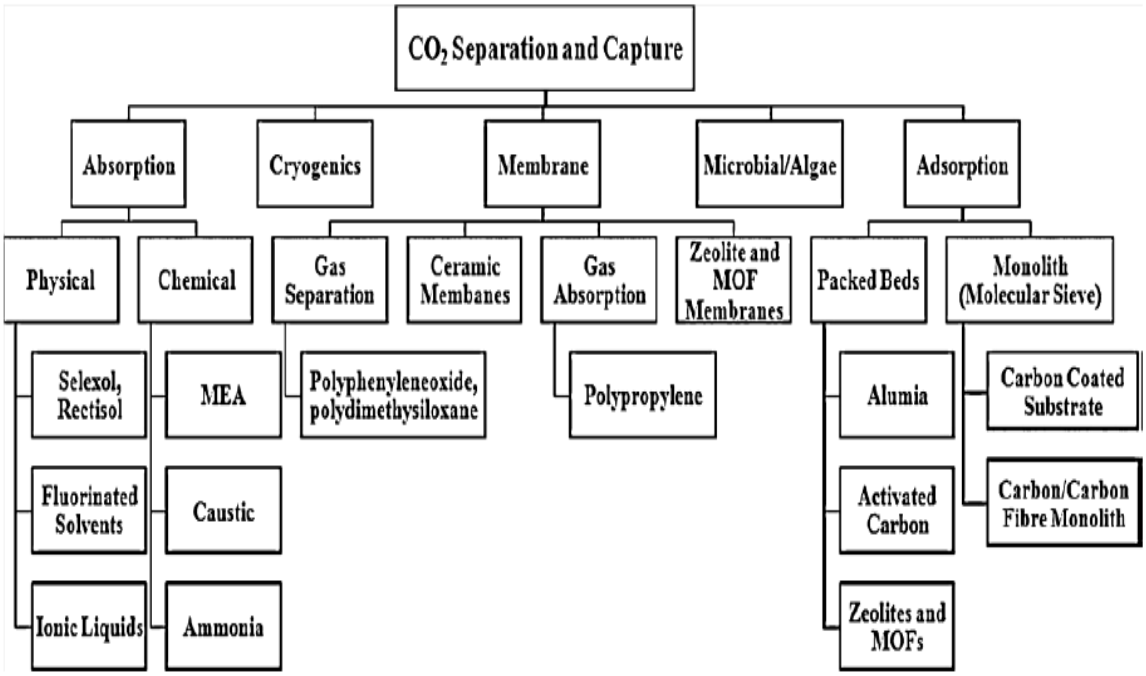

Figure 1.2: Common technologies for natural gas purification [5].

The adsorption process is the adhesion of selective component of the gas in contact with the adsorbent surface. Adsorption process could be classified as physical adsorption and chemisorption. Chemisorption is the chemical bond formation between the sorbate and adsorbent that gives a much larger increase in adsorption volume. In physical adsorption which is more common, the attractive force is weaker than the forces in chemisorption so the heat of physical adsorption is lower hence, adsorbent regeneration is easier as no covalent bond is formed [3]. In a cryogenic separation or low-temperature distillation, low temperature (-73.30 ^{o}C) is used to purify gas mixtures. Cryogenic separations are used commercially for liquefying and purifying CO_2 at relatively high CO_2 concentration.

Generally speaking, physical absorption and chemical absorption process by the reactive solvent in packed towers and the other traditional processes have the advantages of high separation performance and throughput. Nevertheless, the cost of required energy for solvent regeneration, corrosion of the equipment and flow problems caused by a change in viscosity are the drawbacks of these conventional processes. In addition, phase dispersion during the process usually leads to flooding, excessive loading, weeping, foaming, and entrainment [1]. Table 1.3 compares different natural gas sweetening processes.

Table 1.3 comparisons of natural gas sweetening processes [3].

Process	Advantages	Disadvantages
Absorption	Widely used technology for efficient (50-100) % removal of acid gases (CO2 and H2S).	"1-Not economical as high partial pressure is needed while using physical solvents. 2-Long time requirement for purifying acid gas as low partial pressure is needed while using chemical solvents."
Adsorption	"1-High purity of products can be achieved. 2-Ease of adsorbent relocation to remote fields when equipment size becomes a concern."	1-Recovery of products is lower. 2- Relatively single pure product.
Membrane	"1-Simplicity, versatility, low capital investment and operation. 2-Stability at high pressure. 3-High recovery of products. 4-Good weight and space efficiency. .5-Less environmental impact."	1-Recompression of permeate. 2-Moderate purity.
Cryogenic	"1-Relatively higher recovery compared to other process. 2- Relatively high purity products."	"1-Highly energy intensive for regeneration. 2- Not economical to scale down to very small size. 3-Unease of operation under different feed stream as it consists of highly integrated, enclosed system."

1.3 Membranes for CO_2/CH_4 separation:

Clearly, the aforementioned technologies for CO_2 separation from natural gas have serious disadvantages. Alternatively, membrane separation technology has shown enormous potential for CO_2/CH_4 separation. Membranes have drawn a great attention in scientific research area because of its energy efficiency since there is no need for phase transformation like all other process technologies. Besides, the advantages of simple "process equipment, ease of scale-up and module construction, and small footprint make membranes a competitive alternative for the application of gas separation [1]. Consequently, and for long time membrane has been known to constitute mature technologies that have been used in the application of processing natural gas [3].

The performance of the membranes is mainly characterized by two factors. Permeability that measures the gas volume which the membrane could process and selectivity which measures the ability of the membranes to separate different components. Permeability or permeability coefficient (Pe) can be defined as the gas flux transported through the membrane divided by a unit of driving force across the membrane (pressure difference). One can increase the gas volume that the membrane can process by increasing the permeability coefficient, the membrane area, and the pressure gradient across the membrane, or by reducing the membrane thickness [4]. Figure 1.3 presents a Schematic representation of membrane process for the CO_2/CH_4 separation".

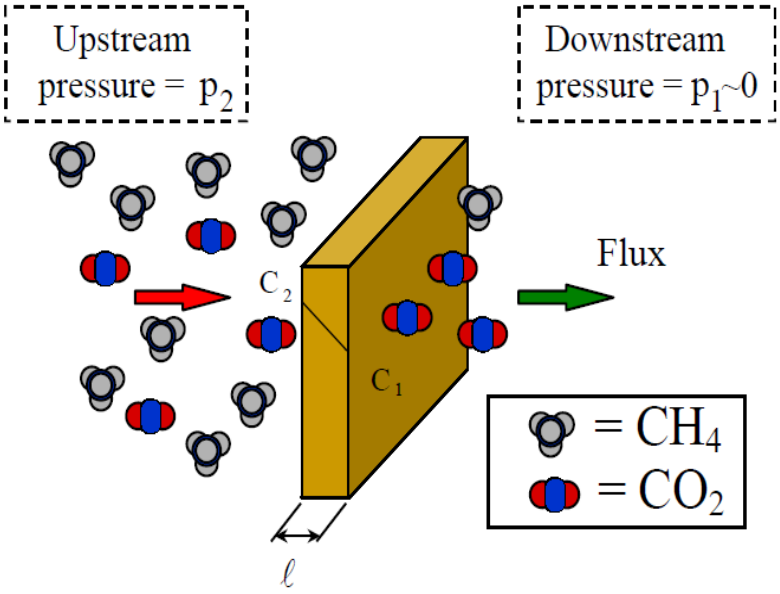

Figure 1.3: "Schematic representation of membrane process for the CO_2/CH_4 separation." [5]

According to the materials that the membrane is made from, gas separation membrane can be generally classified as a polymeric membrane, ceramic membrane, and mixed matrix membrane. The commercial membrane technology employed in NG application is predominantly nonporous polymeric membrane using the solution-diffusion mechanism to separate components.

Polymeric membranes use the pressure difference across the membrane as a driving force to selectively transport CO_2 and not CH_4. The transport mechanism in the polymeric membrane is the solution-diffusion mechanism in which separation of the gas component is based on the differences in the solubilities and /or the mobilities behaviors of the gasses on the membrane". The polymeric membrane could be also classified as rubbery polymer membrane and glassy membrane. Glassy polymer membrane has a rigid structure which separates gasses based on the difference in kinetic diameter of the gaseous and this type of membrane operates below the glass transition temperature.Whereas, rubbery polymer

membrane with elastic and mobile polymer structure operates above the glass transition temperature and hence, the performance of rubbery membranes is based on the differences in the solubility of gaseous species in the polymer. In NG sweetening, glassy polymers have better separation performance than rubbery polymers. Achieving higher permeability without compromising the selectivity is a route to develop new membrane materials for the gas separation application. Broadly speaking, modification of membranes structure in order to increase permeability, unfortunately, results in a reduction of the selectivity (Figure 1.4). Which is a famous trade-off limit for the polymeric membrane. In 1991, Robeson proposed an upper-bound limit for selectivity and permeability of different gasses above which no materials have been recorded to exist. In 1999, Freeman suggested that one should increase the membrane selectivity by interchain spacing and chain stiffness in order to surpass the upper bound. Later on, and in 2008, Robeson again renewed the upper bound with more data from the literature (Figure 1.4). Recently, the 1991 bound has been surpassed by many polymeric materials while few polymers surpassed 2008 upper bound some of them are the cross-linkable 6 FDA duren - DABA co-polyimide grafted with α, β and ɤ cyclodextrin, polymers of intrinsic microporosity (PIM), thermally rearranged aromatic polyimides, poly benzoxazole, microporous polybenzimidazole and poly(benzoxazole-co-pyrrolone). Thus, the trade-off limitation is the main drawback of polymeric membranes [2].

Porous inorganic membranes separate gasses based on molecular sieving or activated transport mechanism. Recently, these membranes have drawn great attention in gas separation because of the high thermal, mechanical and chemical stability, good erosion resistance as well as a long operational life. Even though inorganic membranes overcome

the trade-off limitation of the polymeric membranes on the small scale, much larger costs are required for manufacturing inorganic membranes. Moreover, reproducibility improvement is needed for large-scale production of inorganic membranes [1].

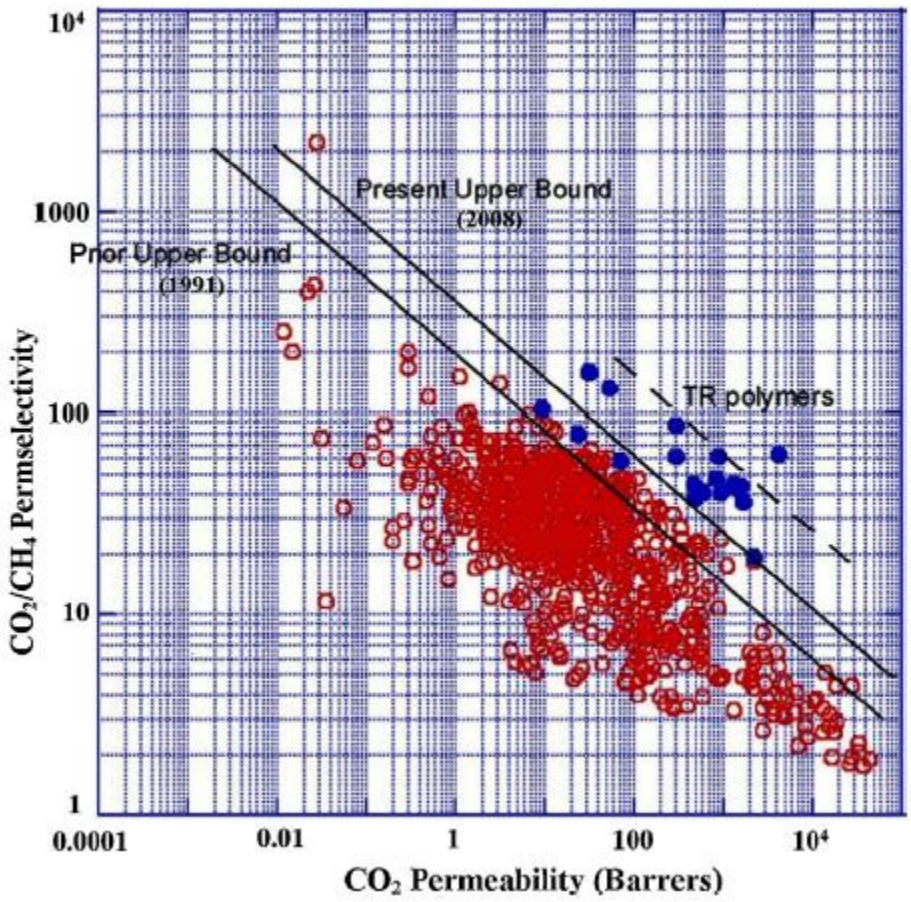

Figure 1.4: Robeson's upper bound curve for the CO_2/CH_4 system [30].

No doubt that the trade-off limitation (upper bound) between permeability and selectivity is the major problem for the polymeric membranes. So, the research scientists have sought to develop a new material and new technique that can push membrane performances to

exceed current Robeson limits. One of the strategies to enhance polymeric membrane performance is to incorporate inorganic material with high sorption capacity or the molecular sieving capability into the continuous matrix (polymeric) phase to fabricate mixed matrix membranes (see Figure 1.5). By combining the advantages of the polymeric membrane (cheapness, simple preparation techniques) with the improved separation characteristics of inorganic materials in a mixed matrix membrane, the separation performance is considerably improved. Nevertheless, mixed matrix membranes synthesis is not a simple task, since the dispersed and continuous phases must be compatible with each other to avoid defects in the membrane and to achieve excellent separation performance.

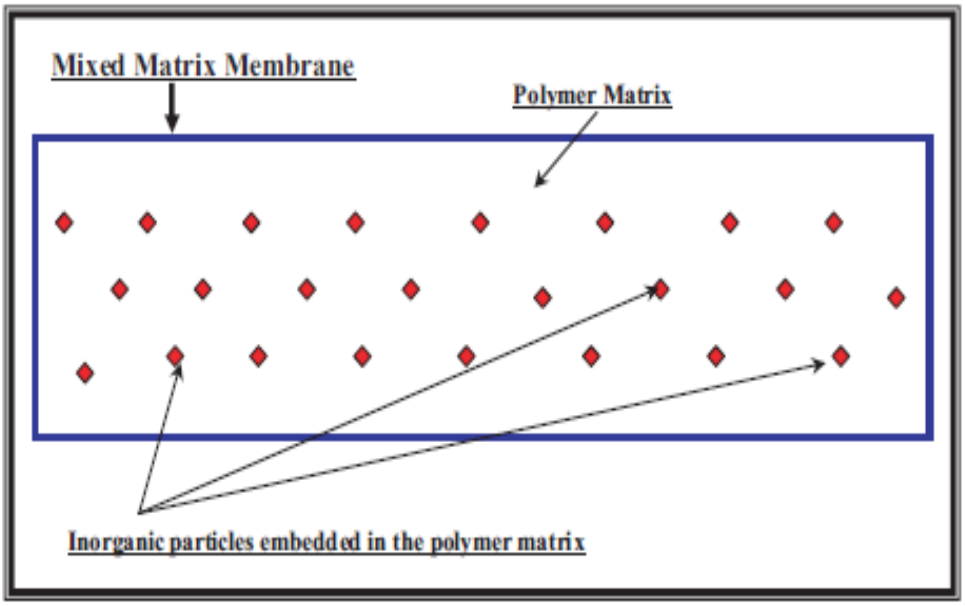

Figure 1.5: A schematic diagram of the mixed matrix with inorganic dispersed phase and continuous polymeric phase [5].

1.3 Thesis objectives:

The main objective of this study is to fabricate a new defect-free carbide-derived carbon (CDCs) /Polyamide thin film nanocomposite membrane for the application of CO_2 removal from natural gas.

The specific objectives of this research are to:

- Prepare a defect-free polyamide membrane using PSF membrane as a support.
- Incorporate CDC nanoparticles into the polymeric film to fabricate the MMMs.
- Characterize and investigate the separation performance of polyamide as well as TFN membranes.
- Study the effect of nanoparticles loading, temperature, pressure, and a number of the selective layer on the separation performance.

CHAPTER 2

LITERATURE REVIEW

2.1 Background on Mixed matrix membranes:

Mixed matrix membrane (MMM) is discovered by UOP research team and can be considered as modified organic membranes. In which micro or nanoparticles of inorganic fillers is embedded into an organic continuous matrix to form a heterogeneous membrane. Powell and Qiao [4], reported that the incorporation of nanoparticles into the polymer matrix could affect the permeability in three different ways:(1) molecular sieving effect to change the permeability, (2) disrupt the membrane structures which results in higher permeation coefficient and (3) they could as well decrease the permeability coefficient by acting as a barrier [1]. Hence, in MMMs the shape selective nanoporous is combined with the processable and mechanically stable organic materials [1]. The materials of dispersed phase in MMMs own specified structures, surface property, and strength. These materials are expected to enhance the polymer membranes performance, however, over the past three decades, not so many attempts to enhance the separation performance of gasses using MMM have been reported due to the difficulties of fabricating mixed matrix membranes. For instance, the poor particles/ polymer adhesion and weak distribution of the inorganic materials in the polymer phase.

MMMs morphology and separation properties are affected by both polymer and dispersed phase. Consequently, selection of materials for the polymer phase and the inorganic fillers are vitally important [5].

The first reported mixed matrix membrane was fabricated by UOP research team. In which silicalite materials were incorporated into cellulose acetate (CA) matrix. Their results demonstrated that the selectivity of O_2/N_2 increased from 3 to 4.3. Moreover, in the mid-1980s and at UOP LLC, CA/silicalite MMMs were fabricated for the application of CO_2/H_2 separation using a feed mixture of CO_2/H_2 (50/50 mol %) at a 50 psi differential pressure. The results revealed that CO_2/H_2 selectivity increased from 0.77 to 5.15 by incorporating the silicalite particles [6].

2.2 Polyamide membranes:

Polyamide membranes are thin film composite membrane prepared by interfacial polymerization techniques. Interfacial polymerization can be defined as a type of step-growth polymerization, in which, the polymerization reaction occurs at an interface between an aqueous solution containing one monomer (polyamines) and an organic solution containing a second monomer (polyacyl halides) [19,5]. Interfacial polymerization is widely used to develop commercial membrane for reverse osmosis [20,21], nanofiltration [22,23], and pervaporation (PV) process.

Generally, the preparation of thin film composite membrane using this method is accomplished by saturation step of a porous support with a water soluble diamine, for instance, meta-phenylene diamine and piperazine followed by a reaction step with an organic diacid chloride solution (such as iso-phthaloyl chloride, trimesoyl chloride) or Vice versa [8]. Figure 2.1 shows Schematic of film growth by the interfacial polymerization reaction. Membranes fabricated using interfacial polymerization techniques have the advantages of the possibility of producing ultrathin skin layer (0.1–1.0 nm) on the porous support, the availability of a large number of monomers that can be

used, and more importantly the defect-free nature and ease to scale-up to the commercial modulus [24,5]. Membranes fabrication using IP for the application of gas separation still lags behind and needs more studies [24,5].

CO_2 removal using facilitated transport membranes has been recognized as one of the routes to enhance the separation efficiency of the organic membranes in order to provide efficient gas separation. CO_2 transport mechanism in membranes containing (primary or secondary) amine functional groups cab be expressed by the following equations [13]:

$$2RNH_2 + 2CO_2 \longleftrightarrow RHNCOOH + RNH_3^+ \quad (1.2)$$

$$2R_2NH + 2CO_2 \longleftrightarrow R_2NCOOH + R_2NH_2^+ \quad (2.2)$$

In these reactions, CO_2 reacts rapidly with the primary or secondary carrier (amine groups) to produce RNHCOO− in the membrane. Moreover, some researchers suggested that in presence of water tertiary amines could play as a catalyst and react with CO_2 as follows [8]:

$$R_3N + CO_2 + H_2O \longleftrightarrow R_3NH^+ + HCO_3^- \quad (3.2)$$

In addition to promoting ion transfer in hydration reaction (Eq.3.2), the presence of water in the membranes can enhance the chain mobility of the polymer matrix and hence higher gas diffusion is expected [8]. Comparing to primary and secondary amines group tertiary amines revealed better gas absorption capacity, higher catalytic efficiency in the hydration reaction, more stability in air, and lower crystallinity [15].

Fixed carrier composite membranes are generally fabricated using solution coating [15,13], plasma polymerization [15,13]and Interfacial polymerization techniques.

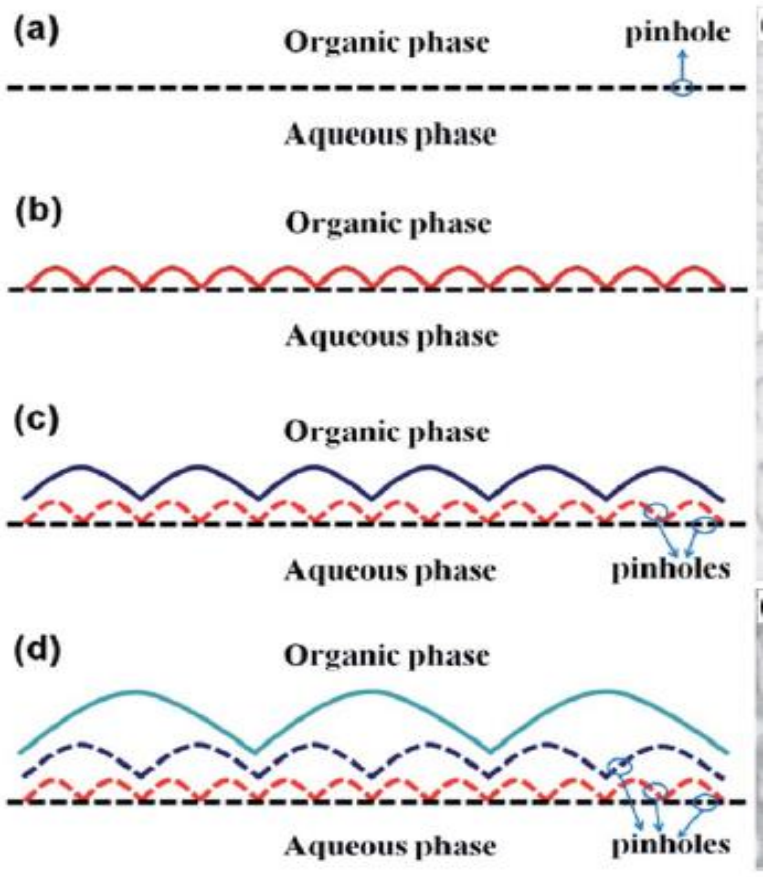

Figure 2.1 Schematic of film growth: (a) formation of a nascent film with uniformly distributed pinholes; (b–d) formation of second, third and fourth generations of bubble-like films [37].

Monomers selection for polymerization reaction is the most important factor affects the separation performance of thin film composite (TFC) membranes. Sridhar et al [14] investigated the performance of PA membrane prepared by interfacial polymerization between MPD aqueous solution and isophthaloyl chloride (organic solution) using polysulfone support. The results showed CO_2 permeance of 15.2 GPU with a CO_2/CH_4 selectivity of 14.4, and for H_2S gas the permeance was 51.6 GPU with H_2S / CH_4 selectivity of 49.1. In another work, Xingwei et al [15] prepared polyamide membrane using

interfacial polymerization between (DNMDAm) and (TMC) using the polysulfone (PS) membrane as a support. The gas permeation tests demonstrated that using DNMDAm (concentration of 0.0062 mol/l) and TMC (0.0226 mol/l) resulted in the highest performance for 20/80 v/v feed gas of CO2/N_2 with 173 GPU permeance of CO_2 gas and CO_2/N_2 selectivity of 70 at a feed pressure of 0.11MPa and 118 GPU permeance of CO_2 for CO_2/CH_4 gas mixture (10/90) with a selectivity of 37.

To the best of our knowledge, in this work it is the first time piperazine and isophthaloyl chloride was used as monomers to fabricate thin film composite polyamide membrane for the application of gas separation.

2-3 Carbide-derived carbon (CDC) nanoparticles:

Nowadays, special carbon element plays a significant role in the chemistry of all living matters. Carbon is also the base of all organic materials. With the advent of nanotechnology revolution, carbon nanomaterials such as nanotubes, fullerenes nanodiamond, nano graphite, carbon onion materials, and nanoporous carbon have triggered increasing attention from scientific researchers. These materials have provided good mechanical, optical, and electrical properties which make them competitive materials in various engineering applications. CNTs (the strongest fiber materials) have been used in membrane fabrication for different applications. Carbon materials can be produced using different routes. For example, ordered graphite is synthesized under very high temperature due to low carbon mobility in its covalent bonded layer. While, diamond is synthesized under conditions such as high pressure, and high energy activation methods [16].

Various carbon structures can be synthesized by selective etching of carbides. Carbide-derived carbon (CDC) is synthesized by extracting metals from metal carbides (Me Cs).. According to preparation conditions nanotube structures with amorphous or crystalline nature, fullerene-like structures, carbon onion, and nano-crystalline diamond can be synthesized. Therefore, all carbon allotropes can be synthesized by removal of metal from metal carbide. Due to layer by layer extraction of metal from the template metal carbide, precise control over the nanoparticles properties can be achieved during the synthesis process and the structure can be modified by controlling the temperature, composition of the environment.

The reaction for CDC production from metal carbide can be described as [16]:

$$MeC\ (s) + 2\ Cl_2\ (g) \rightarrow MeCl_4\ (g) + C\ (s) \qquad (4.1)$$

And by changing the chlorination temperature good control of the pore size and pore size distribution was reported as shown in Figure 2.2.

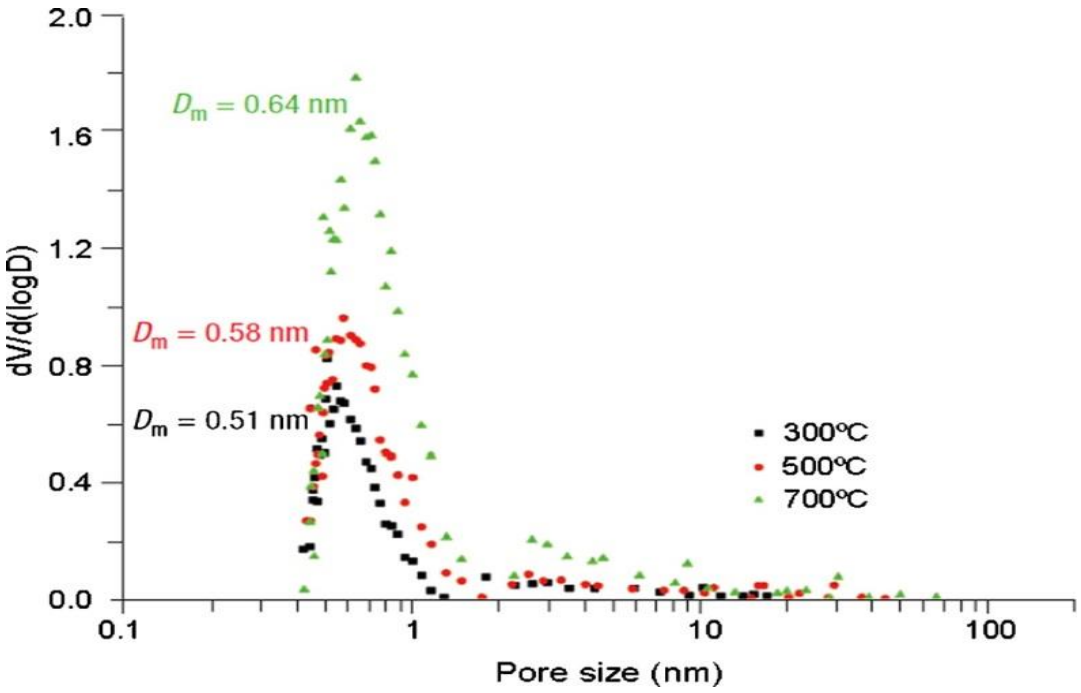

Figure 2.2: Differential pore size distribution at different chlorination temperature [49]

Hoffman et al [16], synthesized a novel carbide-derived carbon membrane by chlorination of TiC precursor at 350 ^{o}C. The resulted carbon layer had a thickness of 500 nm with an amorphous structure. The nitrogen permeability of the prepared membrane was found to be 67 Barrer. Therefore, CDC opens new opportunities to design inorganic membranes with superior separation performance. Moreover, CDC can also be incorporated into organic membranes to enhance its separation performance.

2.4 Filler phase for mixed matrix membranes (MMMs):

As we mentioned above the separation properties and morphology of prepared membranes are greatly affected by organic and inorganic materials used to fabricate MMMs. Filler materials in mixed matrix membranes are classified as porous and nonporous fillers. Metal-

organic frameworks (MOFs family), activated carbon and carbon nanotubes (CNTs) are examples of porous fillers that have been used in fabricating MMMs.

One important factor in selecting a proper filler is the consistency of the pore size distribution and surface property with the gasses. For instance, activated carbon is good for separating CO_2 from CH_4 due to the higher affinity to CO_2 gas. However, activated carbon is not suitable for O_2/N_2 gas system separation. Moreover, 10 ˚A aperture of zeolite 13 cannot act as a molecular sieving materials for oxygen (3.46 A˚ kinetic diameter) and nitrogen (3.64A˚) molecules. While the aperture size of 3.8 ˚A of zeolite 4A discriminates O_2/N_2 gas molecules because of the entropic factors. Therefore, correspondence between molecular sieves and the size and shape differences of the gas molecules must be accomplished to achieve good performance separation. Table.2.1 presents the kinetic diameter of three gas molecules along with other physical properties. However, for nonporous fillers type, the polymer chain segment, and inorganic materials, as well as the functional group's interaction, must be considered. For example, the addition of silica to a polyimide matrix disrupts polymer chain packing hence enhance the permeation of O_2 and N_2 gasses. Whereas, incorporating TiO_2 into polyimide matrix enhances CO_2/CH_4 and H_2/CH_4 selectivity since CO_2 and H_2 interaction with TiO_2 are much stronger than TiO2–CH_4 interaction. In the next few pages, we are going to review the most common and new filler materials that have been used in fabricating MMMs for the application of CO_2 removal from methane [17].

Table 2.2: Gas physical properties including critical properties, saturation vapor pressure at 35 ^{0}C, partial molar volume, and kinetic diameter.

Gas	T_c (K)	V_c (cm^3/mol)	P^{sat} (atm)	$\bar{V}_2$ (cm^3/mol)	Kinetic diameter (Å)
CO_2	304.1	94	81.9	45	3.3
N_2	126.2	86.2	902	48	3.64
CH_4	190.5	98.6	359	46	3.8

2.4.1 Zeolite materials:

Zeolites have the properties of selective size and shape which make them competitive fillers in MMMs for gas separation application [18]. Zeolites have the ability of molecular sieving, in which diffusion of gas molecules with almost equal to or larger size than zeolite particles is difficult to achieve [19]. Nevertheless, MMMs comprising zeolites suffer from the poor zeolites/ polymers compatibility which results in the creation of voids and reducing the performance [20]. SAPO-34 is one of the common types of zeolites that is used in gas separation. SAPO-34 with 3.8 A˚ pore size is well known for selectively passing CO_2 (3.3 A˚ diameters) without CH_4 permeation (3.8 A˚ diameters) [21]. Souha et al [19], developed MMMs by incorporating different SAPO-34 zeolite loading (0 to 10 wt%) into polyetherimide polymer (PEI) using two polymer solvents namely:(NMP) and (DCE) at the room temperature. Using DCE solvent for preparing MMMs resulted in better selectivity. In the fabricated membrane by NMP solvent, SAPO-34 acted as porous materials which increased CO_2 permeance without affecting CH_4 permeance while for DCE solvent because the small solvent molecules entrapped inside the SAPO-34 particles the CH_4 permeance decreased without increasing in CO_2 permeance. The time lag

measurements revealed that CO_2/CH_4 separation was believed to be on gas solubilities base. The gas permeance results demonstrated that at 5 wt% loading of SAPO-34 on the polymer matrix dissolved in DCE, CO2 permeance, and CO_2/ CH_4 selectivity have their highest" value of 4×10^{-10} mol $m^{-2}s^{-1}\ Pa^{-1}$ and 60 respectively. Whereas, using NMP solvent resulted in 2×10^{-9} mol $m^{-2}s^{-1}\ Pa^{-1}$ CH_4 permeance and an ideal selectivity of 12 for CO_2/ CH_4.As a result of increasing SAPO-34 diffusion pathway, CH_4 transport was reduced. Furthermore, there was some agglomeration at 10 wt% filler loading in the membrane matrix. Which indicated creation of defect .Consequently, the gases (both CO_2 and CH_4) permeances increased and CO_2/CH_4 selectivity was reduced. In another work, Hesamoddin et al [21], prepared mixed matrix membrane (MMM) by incorporating SAPO-34 zeolite" into poly amide12bethyleneoxide (Pebax1074) polymer matrix .They investigated the membrane permeability and selectivity for the wide temperature range (25 to 65 ^{0}C) and pressures from 4 to 24 bars. The results revealed that CO_2 permeation increased but CH_4 permeation decreased because CO_2 has molecular size less than the zeolite pore .Which resulted in better CO_2/CH_4 selectivity. For instance, CO_2 permeation enhanced by 33% and CO_2/CH_4 selectivity was doubled at 4 bar and 25 ^{0}C. The enhanced selectivity led to performance of the membrane to pass previous Robeson upper bound and moved toward recent Robeson upper bound. At 20 wt. % filler loading the prepared membrane showed the highest performance with 70% better CO_2/CH_4 selectivity. Owing to zeolite molecular sieve impact, the diffusion selectivity improved without remarkable effect on solubility selectivity. Moreover, comparing with neat membrane, Zeolite /Polymer MMMs have higher solubility coefficients.

Few works studied the LMW additives effect on the Polymer/zeolite membranes for eliminating voids. To investigate the impact of polyethylene glycol LMW additive on the performance of Matrimid®5218/ZSM 5 mixed matrix membranes. Mahsa et al [22], fabricated flat sheet ternary (Matrimid®5218, PEG 20 and calcined ZSM 5) hybrid membranes using film casting technique. PEG acted as the selective LMW CO_2 phallic polymer minimize interfacial defects between the two polymer phase and zeolite materials. FESEM results showed that the ZSM 5 was compatible with the polymer and homogeneous dispersion of ZSM 5 at low PEG (less than 5 Wt. %) content while for 15 wt% PEG content, there was an agglomeration of nanoparticles and pores were formed in the dense polymer. The characterization results revealed that there were PEG / ZSM-5 hydrogen bonds. In addition to, the stronger PEG / ZSM-5 hydrogen bonds than PEG-Matrimid led to a greater tendency of PEG/ ZSM-5 interaction. Furthermore, embedding the zeolite into Matrimid/ polyethylene glycol polymer reduced the crystallinity due to larger intermolecular distance in the polymer chains." The gas permeation results demonstrated that at 5 wt.% loading of ZSM 5 in the polymer with 5 wt.% content of PEG, CO_2 permeability enhanced from 7.68 (for pure Matrimide) to 11.53 Barrer and CO_2/CH_4 selectivity also increased from 34.9 to 60.1 which are 50% and 72% better permeability and selectivity compared to the pure Matrimid. This improvement was attributed to the CO_2-philic properties of adding a low amount of PEG as well as the embedding of low loading ZSM-5 which provided accessible channels and favorable intermolecular attractive forces between the CO_2 and ZSM-5 particles.

Asymmetric Matrimid/ZSM-5 mixed matrix membranes were investigated for CO_2/CH_4 separation application by Fatereh et al [20], size selective ZSM-5 zeolite type with 50"

Si/Al ratio was used which render the zeolite with more hydrophobic properties to enhance the filler/ polymer compatibility. The results showed that incorporating 6 wt % loading of ZSM-5 in the matrix membranes resulted in better CO_2/CH_4 selectivity and gas permeance increased from 5.1 GPU for neat Matrimid to 6.6 GPU. Nevertheless, the gas permeance tests showed that for high (30 wt. %) filler loading the gas permeation improved and the CO_2/CH_4 selectivity decreased.The decline in the selectivity was attributed to the polymer/ZSM-5 particles interfacial void formation resulted from the higher filler loading. Furthermore, the best Matrimid/ZSM-5 membrane performance reported as 14.5 GPU of CO_2 permeance and 15.6 of CO_2/CH_4 selectivity. The investigation of the pressure and temperature effects on the separation performance revealed that the permeance of CO_2 declined with an improvement in the CO_2/CH_4 selectivity when the feed pressure raised from 3 to 12 bar, in addition, increasing the temperature from 35 to 65 ^oC showed an increase in gas permeance along with declining in the CO_2/CH_4 selectivity.

2.4.2 Metal-organic frameworks (MOFs):

MOFs are organic–inorganic porous materials tailored by connecting metal complexes with organic linkers to obtain tunable pore geometries and flexible framework. MOFs have attracted strong attention over the past few years since they possess large surface areas, well-defined pores, superior thermal/chemical stability, and well-proportioned pore sizes. Yehia et al.[23], introduced the first MOF/MMMs by embedding copper (II) biphenyl dicarboxylate-triethylendimine as filler in PAET for gas separation. Their results revealed that CH_4 permeability increased for 20–30 wt. % filler loading. Nevertheless, a decrease in CO_2/CH_4 perm-selectivity was observed. Which was attributed to an increase in hydrophobicity of the MMM, which increased the adsorption of methane in the copper

filler. Nowadays, these membranes can easily surpass the Robeson's upper limit by proper selection of MOF-polymer couple.

Basu et al. [23], fabricated PDMS membranes containing various fillers such as MIL 53(Al), MIL 47(V), HKUST 1 and ZIF-8 for nanofiltration. This work is the first to use flexible MOFs in MMMs. One year later, Basu et al. [11], synthesized similar MMMs by embedding MIL-53(Al), ZIF-8 and HKUST 1 in Matrimid® for separation of CO_2 from various gas mixtures. They showed that with a 0–30 wt. % filler loading, "HKUST-1, and MIL-53(Al) revealed superior selectivity compared with ZIF-8. Additionally, they claimed that this result was attributed to the strong CO_2 interactions with the unsaturated metal sites for HKUST-1, and interactions with the hydroxyl groups of MIL-53(Al) and its breathing behavior.

In another work, Zornoza et al. [24], synthesized nanosized NH2-MIL-53(Al) (amino functionalized MIL-53) crystals with a narrow size distribution and incorporated them into polysulfone Udel®(PSF) polymer. Their results demonstrated that high-level loading was achieved (up to 40%) due to the hydrogen bonding interactions between MOF and polymer. In other words, outstanding compatibility between sulfonic groups of the polymer and the surface amine moieties of the filler was attained. Breathing effect was the key factor for CO_2 separation. For instance, the contribution of filler was almost negligible when the CO_2 pressure is low, while, at a higher CO_2 pressure, these MMMs exhibited a high CO_2/CH_4 selectivity. It must be noted that this behavior is opposite to the typical intrinsic property of polymeric membranes. Furthermore, increase in the selectivity at higher pressures plays an important role for natural gas and biogas upgrading, because the retentate has to be kept pressurized in these applications.

ZIFs constitute a zeolite-like subclass of MOFs that have attractive properties in comparison with other MOFs such as higher thermal (up to 400^{o}C), chemical, and moisture stability [25]. These particles are commonly constructed by connecting metal clusters such as Co and Zn using functionalized imidazole linkers, which provides solids of exceptionally small pores, displaying zeotype architectures such as SOD, RHO or LTA, among others. Díaz and co-workers [26], fabricated novel MMMs by incorporating 10, 20 and 30 wt.% Zn (2-methylimidazole) (ZIF-8) into PPEES. The gas permeation results demonstrated that CO_2 adsorption was enhanced as ZIF-8 loading increased. In a similar work, Ordonez et al. [27], performed a series of experiments for the permeation of various gasses across the ZIF-8/Matrimid® MMMs with filler loadings of up to 60 wt.%. Their results indicated that at 40 wt. % loading, CO_2/CH_4 selectivity was considerably enhanced, but by increasing the loading to 50–60 wt. %, the selectivity decreased due to the ZIF-8 aggregation. They attributed the increase in permeability (up to 40 wt. %) to the presence of extra polymer free volume that increases the distance between polymer chains, resulting from the addition of ZIF-8 to the glassy polymer. Song et al. [28] evaluated ZIF-8/Matrimid® at lower contents of filler (up to 30 wt.%). Their results confirmed outstanding adhesion between polymer/filler. Additionally, CO_2 permeability increased drastically while CO_2/CH_4 selectivity did not increase upon an increase in ZIF-8 loading. This may be due to the increase in the free volume of polymer in the presence of ZIF-8 and the free access of gas to ZIF-8 cages. Yang et al[27], extensively studied CO_2 and H_2 permeation properties of ZIF-7/PBI MMM at high loading levels (up to 50 wt.%) of ZIF-7. The results exhibited that H_2 permeability increased along with enhancement of H_2/CO_2 selectivity at high temperature (up to 180 ^{o}C). Bae et al[25], synthesized ZIF-90 particles

and embedded them into three different PIs polymers (Ultem®, Matrimid ®, and 6F DA-DAM). The MMMs, particularly ZIF-90/6FDA-DAM MMM, exhibited great performance due to the properly selection of functionalized filler that was embedded in a high flux polymer. The results of Ultem® and Matrimid® MMMs exhibited considerably enhanced CO_2 permeability without any loss of CO_2/CH_4 selectivity". In contrast, CO_2/ CH_4 perm-selectivity of ZIF-90/6FDA-DAM showed significant enhancement possibly due to the better adhesion between ZIF-90 and6FDA-DAM than Ultem® and Matrimid® polymers.

2.4.3 Carbon nanotubes (CNTs):

To study the synergetic effect of combining nanofillers. Xueqin et al [29], incorporated CNTs and GO into a Matrimids matrix to fabricate the MMMs for CO_2 separation.The gas permeation tests demonstrated that using only carbon nanotubes as fillers resulted in high CO_2 permeability due to the extraordinary smooth nanotubes and large carbon nanotubes pores. This higher permeability was accompanied by decreasing in the CO_2/CH_4 selectivity. Nevertheless, owing to the agglomerations of nanoparticles at high (10 wt %) filler loading, the gas permeability decreased. Moreover, graphene oxide based MMMs have high CO_2/CH_4 selectivity and low CO_2 permeability. The good selectivity was due to decrease the chains mobility. The combination of the two fillers brought about a good synergistic effect on the separation performance. At total fillers loading of 10% (5wt % of CNTs and 5wt % of GO) the CO_2 permeability has the highest value of 38.07 Barrer with a CO_2/ CH_4 selectivity of 84. Comparing to Matrimids membrane, these values are 331%, higher in CO_2 permeability and 149% in CO_2/CH_4 selectivity. The enhanced separation performance was attributed to CNTs pathways which improved the gas permeability

besides. The better selectivity from the presence of hydroxyl and carboxyl groups of graphene oxide surface.

Luca et al [30], embedded amino-functionalized multi-walled carbon nanotubes into crosslinked polyvinyl alcohol polysiloxane/amine solution to fabricate mixed matrix membranes using solution casting method. They studied the performance of the membrane under high pressures (15 bar to 28) and temperatures between 103 and 121 ^{o}C along with different fillers loading. Incorporating the amino-functionalized multi-walled nanotubes into the matrix brought formation of nano-reinforced facilitated transport that significantly enhanced the separation performance besides, improving the membrane stability at high pressure. The gas permeation tests at 107 ^{o}C and 15 bar showed an average permeability value of 957 Barrers along with CO_2/ CH_4 selectivity of 264.

The commercialize Elvaloy4170 polymer was studied for the first time in MMMs for gas separation by Fatemeh et al [31], they incorporated multi-walled carbon nanotubes into the Elvaloy4170 to fabricate the MMMs and investigated the impact of acid functionalized MWNTs and their loading on the gas separation performance and the morphology. DSC analysis revealed that as the F-MWNTs loading increased the membrane glass transition temperature.Which indicated an excellent interfacial interaction resulted in the formation of a rigidified polymer at the interface with restricted chains movement. FESEM images showed that with 1 and 2 wt % loading a good dispersion in the matrix for both R-MWNTs and F-MWNTs was achieved. Nevertheless, cross-section images demonstrated that at 4 wt. % fillers loading there was a formation of R-MWNTs agglomeration whereas, F-MWNTs dispersed homogeneously. This phenomenon confirmed that to avoid nanotubes aggregation and to have a good interfacial adhesion the functionalization of MWNTs was

an effective approach. The gas permeation results demonstrated that for an increase in the pressure from 2 to 6 bar a 30% improvement in the CO_2 permeability (with a value of 104 Barrer) and 14% in CO_2/ CH_4 selectivity (value of 7.5) were achieved. Moreover, in comparison with the neat membrane, at a 1wt.% loading of functionalized -MWNTs, CO_2 and CH_4 permeabilities enhanced by 30% and 40%, respectively. Furthermore, CO_2/CH_4 selectivity was increased with increasing the F-MWNTs content from 1wt % to 4wt % in the MMMs. The results also showed that the selectivity of the MMMs reduced with increasing the loading of R-MWNTs. However, it enhanced as a function of the functionalized -MWNTs loading.

2.4.4 Carbon molecular sieve (CMS):

Carbon molecular sieve is characterized by the pore size distribution and it discriminates gasses which have slight different kinetic diameters. This material has hydrophobic internal surfaces and it has the ability to separate air by O_2 adsorption as well as removing carbon dioxide from landfill gas. Rizwan et al [32], fabricated MMMs for gas separation using N-Methyl-2-pyrrolidone (NMP) as a solvent via evaporation method. To fabricate the MMMs they incorporated carbon molecular sieve (CMS) into polyethersulfone (PES) with different filler loading (10 and 30 wt. %). The characterization results demonstrated that the mixed matrix membranes have good compatibility between the CMS particles and the polymer chains within 51.37μm to 67.68μm thickness range. Moreover, the filler particles dispersed uniformly at low loading but there was an agglomeration of CMS at higher filler loading. Owing to the addition of CMS the thermal stability was enhanced. The gas performance experiments showed that as the filler loading "increased the CO_2 permeability

and CO_2/CH_4 selectivity improved. At 2 bar pressure, the CO_2 permeability increased from 50.86 GPU to 122.20 GPU and CO_2/ CH_4 selectivity improved from 3.08 to 10.33.

2.4.5 Silica materials:

Asim et al [33], incorporated COK-12 silica nanoparticles into polyimide (Matrimid) to fabricate MMMs for gas separation. The filler materials have a 2-dimensional hexagonal structure with narrow pores. SEM analysis showed that the filler dispersed well in the polymer matrix.Moreover, Owing to the higher diffusion of penetrant gas molecules the experiments tests showed improvements in the gas permeation along with reducing the trend of activation energy of gas molecules with increasing the filler. However, the ideal and mixed-gas selectivity decreased slightly at higher filler loadings. Sunghwan et al [34], prepared MMMs by embedding (DMS) into two polymer matrices, namely,6FDAM:DABA (3:2) and polysulfone. They investigated the single permeabilities of the MMM.The results revealed that for both membranes (6FDA DAM: DBA (3:2)- and PSF- based MMM) at a 0.2 weight fraction of nominal DMS, gas permeabilities significantly improved as a result of the diffusivity enhancement. Which attributed to the three-dimensionally interconnected DMS pore structures. Moreover, due to the difference in the degree of rigidification of polymer chains around the particles", the DMS/ 6FDA-DAM: DABA MMMs has greater improvement in permeability compared with the DMS/ PSF matrix. Uniformed size and shape silica particles have great contribution in composite materials, enhancement and controlling of the properties of the particles tailored for specific applications can be accomplished through surface functionalization of the silica particle [35].

Shirin et al [36], investigated the feasibility of fabricating PEBA-nano silica membranes for CO_2 permeation using aminopropyl-tetraethoxysilane (APTES) as a precursor through a sol-gel process. The results demonstrated that the CO_2 permeability enhanced with pressure for both pure PEBA (from 89.7 to 96.1 barrer) and PEBA-10 wt. % nano silica membranes (from 76.3 to 82.1 barrer), the increase in the permeability was owing to the higher solubility along with greater driving force. Furthermore, the pure PEBA membrane has higher gas permeability than PEBA-10 wt. % nano silica membrane due to filling the free volume between the polymeric chains of the nano silica particles. In other work, Ali et al [37], investigated the separation performance of SiO_2 nanoparticles incorporated into PEBA (grade 1657) membrane with different SiO_2 nanoparticles contents. They performed a chemical surface modification of the nanoparticles using cis-9-octadecenoic acid (OA) to achieve excellent dispersion of SiO_2. The results showed that as the nanoparticles loading increased (from 0% to 8%) the ideal permeation selectivity value enhanced from 9, 18 and 55 to 17, 45 and 124 for CO_2/ H_2, CO_2/ CH_4, and CO_2/N_2, respectively.

Waqas et al [35], prepared carbon–silica nanocomposite (CSM) fillers by using hard template synthesis technique, then CSM embedded into the Matrimid membrane to fabricate series of MMMs using phase inversion technique. The formation of defect-free membranes was achieved by control the evaporation of the solvent after casting process. The separation performance results showed an improvement in the performance by the existence of the carbon phase in the MCM-41 particles provided that the affinity for the CO_2 gas molecules was increased, besides the presence of higher free volume within the membrane. For a 50:50 feed composition of (CO_2/N_2 and CO_2/CH_4) gas mixtures , these MMMs resulted in a considerable improvement in the separation performance of CO_2 from

N_2 and CH_4 leading to a 600 % improved permeability (up to 27 Barrer) combined with 65% improvement in the selectivity (up to 42.5) for the CO_2/N_2 gas mixture.

2.4.6 Nano clay:

One-dimensional (1D) clay minerals are not well studied and have drawn less attention. The (1D) clay mineral Sepiolite with two tetrahedral silica sheets in between a magnesium oxide hydroxide sheet with $Si1_2O.30Mg.8(OH)_4$ $(H_2O)_4$ $.8H_2O$ as the unit cell formula composites [38]. Montmorillonite (MMT), is a kind of swelling clay, which is cheap and natural forming. Montmorillonite (MMT) has been employed predominantly in polymer-clay nanocomposite synthesis [39]. Mansur et al [39], fabricated three different types of asymmetric flat sheet membranes using phase-inversion method: PSF membrane, PSF/MMT MMMs, and surface modified PSF/O.MMT MMM. The characterization studies revealed that the thermal stability of the PSF /MMMs was better than the neat PSF membrane. Furthermore, the study proved that the morphology of the MMM affects the thermal stability. According to their results, Mansur et al [39], expected that PSF/MMT MMM have better selectivity and permeability in comparison with the neat polymer membrane whereas, PSF/O.MMT is expected to have good permeability and lower selectivity. In conclusion, PSF is not compatible with surface modified MMT with 25-30% of methyl hydroxyethyl hydrogenated tallow ammonium. The results also showed that higher nano-clay loading contributed to significant agglomeration, even thought, better adhesion between the polymer and nano-clay was achieved. In another work, Rezaei et al [40], investigated morphology, structure, gas permeability, wetting resistance, and mechanical stability of Porous hydrophobic PVDF hollow fiber MMMs with different hydrophobic MMT contents. The results showed that finger-like macro voids formation

was enhanced with the incorporation of the clay and reduction in the viscosity of the spinning dope caused the surface porosity to increase. Moreover, when 5 wt. % MMT nano-clay was added the surface roughness was increased and the surface hydrophobicity enhancement considerably hence high wetting resistance LEPw, and absorption flux were achieved. The long-term contractor test demonstrated that the un-wetted membrane behavior and the absorption flux was constant over 350 h.

2.5 Polymer phase for mixed matrix membranes (MMMs):

Traditionally, both rubbery and glassy polymers have been used for preparing the polymer phase in MMMs for CO_2 removal application. The rubbery polymers have a flexible polymer chain structure which provides the ability of chain segments rotation around the main chain bonds. Whereas, glassy polymers, have rigid chain structure without segmental motion.

As stated before, for MMMs to have reasonable separation performance the polymer and dispersed phases must have good adhesion. The rubbery polymers have strong interactions with filler materials which lead to the formation of defect-free membranes. Nevertheless, the high mobility of rubbery polymers lead to the highly permeable membrane, and thus, the organic matrix will dominate the gas transport in the membrane without the considerable effect of the dispersed particles on the transport. In contrast, for glassy polymers with rigid chain structures provide superior separation performance, however, these structures weaken the polymers/particles interactions. Consequently, defects at the interface are observed in the MMMs prepared using glassy polymer and that compromise the performance properties of the membrane. Generally speaking, a glassy polymer that has high selectivity is preferred to a rubbery polymer with high permeable but poor

selective. Nevertheless, owing to the rigid structures the adhesion between the polymer phase and the dispersed particles is a challenging problem for using glassy polymers to fabricate defect-free mixed matrix membranes.

Ahn et al [5], fabricated glassy polysulfone mixed matrix membrane to investigate the transport properties of the glassy polymer. Their results demonstrated that higher silica content resulted in higher gas permeability as a result of the much higher free volume between the polymer matrix and silica fillers [41].

Recently, few papers have talked about a new family of polymers called block copolymers that contains both rigid and soft polymer segment, hence potentially enhancing the adhesion strength between the polymer and the particles. In one work [17], incorporation of carbon nanotubes and zeolite-L into Copolymers [poly(imide siloxane)] has shown good copolymers /filler compatibility.

Reverse selective polymer like PM-P, PT-BA, and PTM-SP are a new class of polymer used in mixed matrix membrane. These polymers have unique favored transport of CO_2 over smaller gasses and the CO_2 permeability improves with increasing the size of the side groups. Fractional free volume can be presented from the isopropyl groups as well as from substituting the methyl group on the carbon of PM-P and PTM-SP. Which leads to solubility controlled transport mechanism instead of the diffusivity controlled mechanism. Consequently, CO_2 exhibits higher permeability than the other smaller gas molecules.

The properties of the polymer material greatly affect the morphology of the MMMs. One strategy to enhance the adhesion (between the polymer/particles) is the use of an external linker, for example, silane coupling agent, however, this additional agent may result in pore blocking problem. So, polymer material along with integral chemical linkage which is

intrinsically part of the chain backbone may enhance the adhesion and prevent the pore blockage at the same time. This route was studied by Manouns et al [5] when they formed a fluorinated polyimide from 6 FDA 6FpDA/ 4 MPD/ DA-BA using carboxylic group on the chain. H_2 bond or even covalently bondable sites for interaction could be provided by the presence of the carboxylic groups can provide with the particle surface. The chemical ligands help the polymer to not be completely detachable from the particle surface and thus resulting in better adhesion with enhanced membrane morphology.

In conclusion, MMMs are a new promising generation of membranes not only for CO_2 separation but also for many other applications. Incorporating different inorganic materials as inexpensive fine fillers modify the separation performance of conventional polymeric membranes. Thus, MMMs will remain as a key research area for improving polymeric membrane performance in different aspects. For instance, investigation of new filler materials with good properties and using nanomaterials with a shape other than particles (CNF for example). In order to fabricate MMMs with superior properties, the following key aspects should be considered: the proper selection of solvent, filler and the polymer matrix and matching transport properties of the two phases. Polymer flexibility and promotion of polymer rigidification during membrane formation and also the promotion of molecular adsorption of the polymer onto the inorganic surface are also important in the preparation of MMMs. Over the past few decades, a comprehensive study has been done with a huge database in gas separation using mixed matrix membrane techniques. However, fully exploring new nanoparticles to use in the under-developed MMMs is a critical concern.

In order to develop and investigate new inorganic materials for MMMs fabrication. CDC (Carbide-derived carbon) was used in this study. Carbide-derived carbon (CDC) prepared from chlorination of metal precursor (carbide) is a new class of nonporous material that has promising features in gas separation. Moreover, these materials could be produced at narrow pore size distribution, tuned pore size (0.5–3 nm) and surface chemistries, high surface area per unit mass (up to 3000 m^2/g), and excellent mechanical properties. Therefore, this package of good properties makes CDC a competitive material for CO_2 separation. To the best of our knowledge, this is the first time CDC materials will be incorporated into a polymeric membrane to fabricate a Mixed Matrix Membrane for carbon dioxide separation.

CHAPTER 3

EXPERIMENTAL METHODOLOGY

3.1 Introduction:

This chapter covers the materials and methods employed to develop the thin film nanocomposite membranes. Moreover, the experimental techniques used to characterize the fabricated TFC and TFN membranes are discussed. Section 3.2 talks about the materials used for preparing PSF support, polyamide composite membrane, and thin film CDC/polyamide membranes. The preparation procedure is discussed in details in section 3.3. Detailed Characterization of CDC nanoparticles, PSF, polyamide, and CDC/Polyamide membranes are covered in section 3.4. Finally, section 3.5 presents the experimental method we used to evaluate the separation performance of the fabricated membranes.

3.2 Materials:

Polysulfone pellets (Mw of 35000) were purchased from Sigma–Aldrich Chemical Co and used as a substrates polymer. N, N-dimethylacetamide (DMACs) (99.9%) was used as a less volatile solvent, tetrahydrofuran (THF) (99.9% inhibitor free) was the primary volatile solvent and absolute ethanol (EMSURE) was selected as a non-solvent additive. Piperazine (P45907, 99%) and Isophthaloyl chloride (IPC) were purchased from Sigma–Aldrich Chemical Co and used as the monomers for IP reaction. Methanol and N-hexane (96% Schlau) were purchased from Fisher Scientific Canada. Carbide derived carbon

nanoparticles were synthesized and provided by in Dr. Isam Aljundi with the characteristics shown in Table 3.1

Table 3.1: Different structural properties of the prepared CDC compared to untreated TiC powder

Sample	BET Surface area (m^2/g)	Langmuir Surface area (m^2/g)	$A_{micropor}$ (m^2/g)	$A_{external}$ (m^2/g)	V_t (m^3/g)	V_{micro} (m^3/g)	V_{meso} (m^3/g)	Avera gepore size (nm)
Untreated TiC powder	39	128	7	31	0.051	0.002	0.049	-
CDC	2589	3651	1827	323	1.216	0.873	0.343	1.542

3.3 Membrane preparation:

3.3.1 Polysulfone support:

PSF support was fabricated by the dry/wet phase inversion technique. Prior to membrane preparation, the polysulfone polymer particles were dried overnight at 100 ^oC in a vacuum oven in order to completely remove the moisture from the polymer. PSF pellets were dissolved in a mixture of N, N-dimethylacetamide (DMACs) and tetrahydrofuran (THF), then ethanol is added and the solution was stirred for 24 h at 25 ^oC in a magnetic stirrer. The composition of the solution is shown in Table 3.1. The dope solution was then degassed at room temperature for 24 h to remove air bubble. After that, the solution was casted on a clean glass plate with a thickness of 200 μm using a casting knife. The membrane was left at air for 60s at ambient condition and subsequently immersed in a DI water coagulation bath for 24 h. The prepared membranes were finally immersed in methanol for 2 h for solvent-exchange post treatment and treated with PDMS (3% in

hexane) to eliminate infinitesimal defects or pinholes in the membrane and then dried in vacuum oven for 48 hr.

Table 3.2: Composition and amount of dope solution.

Component	Amount(g)	Concentration (%)
PSF Pellets	4	23.12
DMAC	5.81	33.44
THF	5.81	33.44
Ethanol	1.75	10

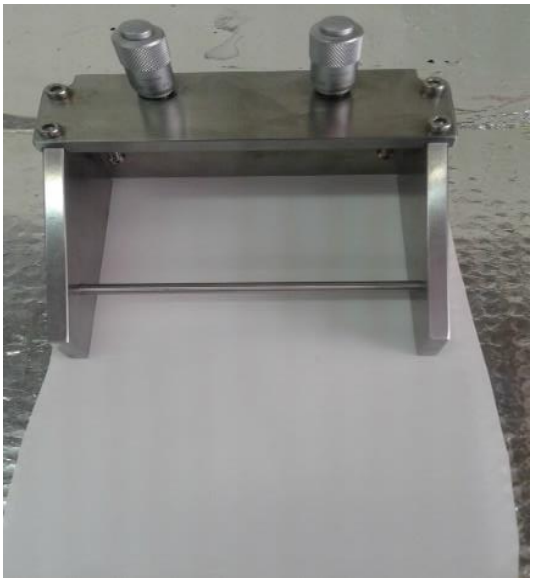

(a)

(b)

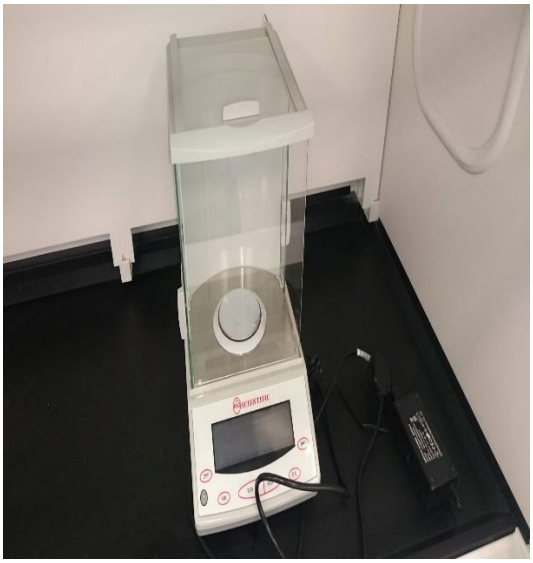

(c)

(d)

Figure 3.1: Equipment used in fabricating membranes (a) casting knife machine, (b) Magnetic stirrer with temperature controller, (c) Electronic balance and (d) Polysulfone pellets.

3.3.2 Polyamide preparation:

Polyamide membrane was prepared using interfacial polymerization (IP) method in which a polymerization reaction occurs between an aqueous solution and an organic solution. Isophthaloyl chloride (IPC) in hexane solution was used as the organic phase and Piper zine in DI water was the aqueous solution the reaction is shown in Figure 3.2. PSF support was saturated with Piper zine solution (2%w/v) for 10 minutes after that the excess solution a plastic roller was used to remove excess solution. Subsequently, the support immersed in the reaction solution (0.2%w/v Isophthaloyl chloride IPC) for 3 minutes and the excess unreacted IPC was removed using pure hexane. Finally, the membrane was dried at 80 ^{o}C for 10 min and the fabricated polyamide membranes were kept in DI water. For thin film nanocomposite membrane, CDC nanoparticles were added to the organic phase (IPC) and the mixture was sonicated for 15 minutes using prop sonicator and then the interfacial polymerization reaction was conducted.

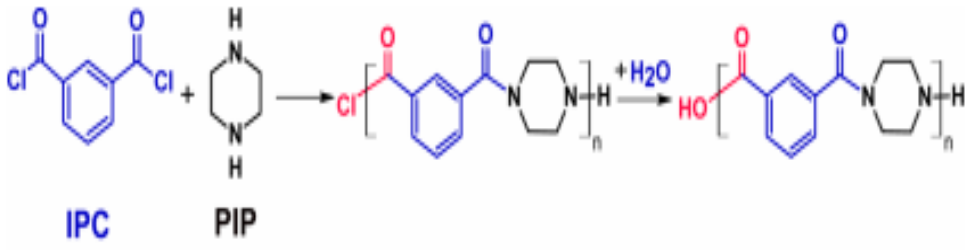

Figure 3.2: Polymerization reaction between piperazine and isophthaloyl chloride (IPC) [69]

Figure 3.3: The vacuum oven for drying polymer pellets and the fabricated membranes.

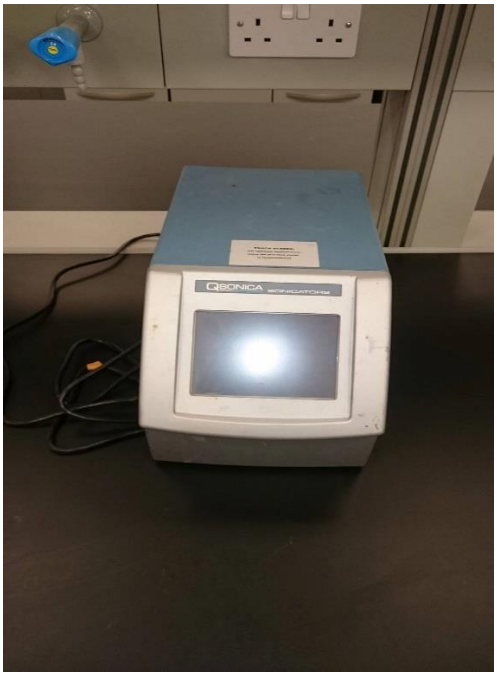

Figure 3.4: probe sonicator

Figure 3.5: Oven for drying membranes

3.4 Membrane characterization:

The fabricated polyamide membrane, as well as CDCs/polyamide mixed matrix membranes, were characterized by SEM, FT-IR, TGA, and XRD analyses to study the chemical structure, surface morphology, thermal stability, and crystallinity.

3.4.1 Scanning Electron Microscopy (SEM):

Scanning electron microscope SEM images were taken to study the surface morphology of the CDC nanoparticles, PSF support, polyamide surface as well as the thin film nanocomposite membrane (TFN). To take SEM images, gold layer with a thickness of 5 nm was used for coating the membrane samples by an Ion sputter coater Q150R S (Quorum Technologies) in Figure 3.7. SEM (Tescan, MIRA 3 LMU FTIR) operates by generating high electron energy from the electron gun. After that one or two condenser lens are used to condense the beam of the electron. Followed by producing a magnetic field and deflecting electron beams back and forth by using scanning coils. The electron beam focused on the specimen and scan the required location of the sample. Figure 3.6 shows SEM set-up.

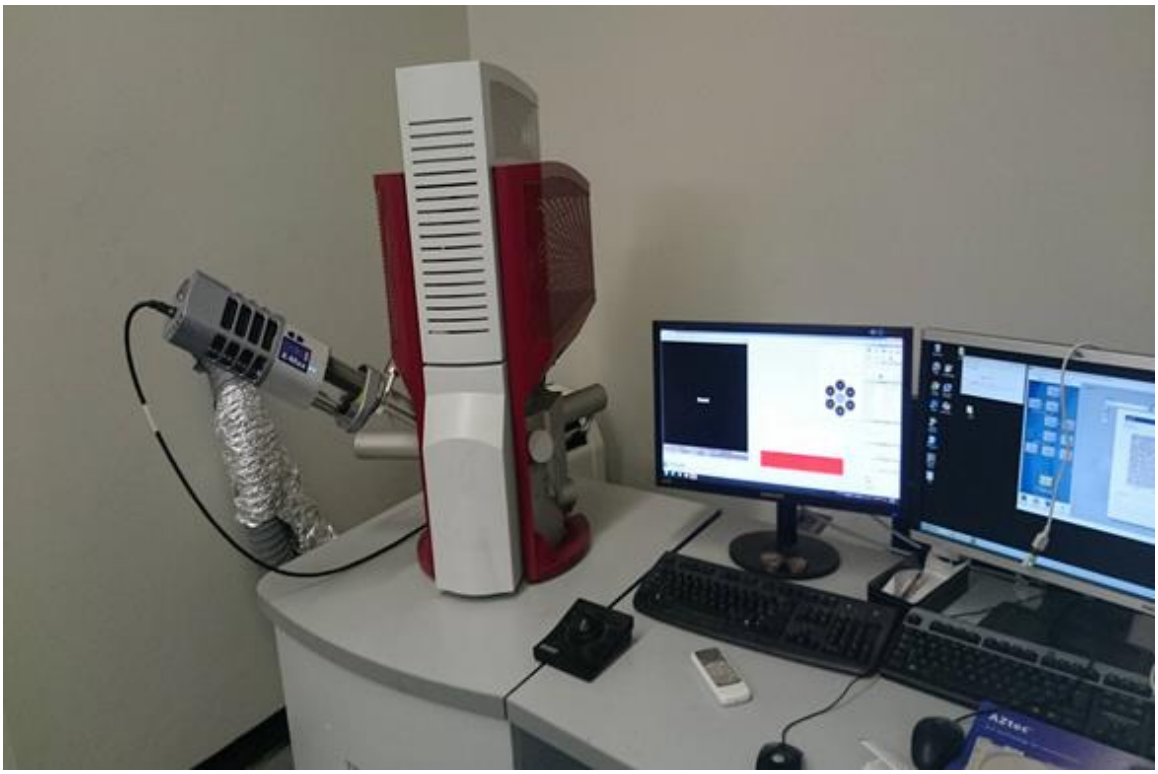

Figure3.6: Scanning electron microscope (SEM) set-up.

Figure 3.7: Ion sputter coater Q150R S (Quorum Technologies).

3.4.2 Fourier transformation infrared (FT-IR):

Fourier transformation infrared (FT-IR, (Nicolet 6700) spectroscopy) in Figure 3.8 was used to investigate the chemical structure of the fabricated Polyamide composite layer and the polyamide /CDC nanoparticles layer with different amount of filler loading.

Figure 3.8: Fourier transformation infrared (FT-IR, (Nicolet 6700) spectroscopy).

3.4.3 X-ray diffraction test:

XRD (Bruker D8-Advance X-ray diffractometer) analysis was applied to PA membranes to get information about the crystallinity and amorphous nature of the fabricated polyamide membrane composite layer and the effect of incorporating CDC nanoparticles on the crystallinity of the fabricated membranes layer with different amount of filler loading.

3.4.4 Thermogravimetric analysis (TGA)

Thermal stability of fabricated polyamide – polysulfone thin film composite was examined by thermogravimetric analysis (A Netzsch model STA 449 F3 Jupiter ® TGA in Figure 3.10) in the temperature range of 30–800 ºC at a heating rate of 10 ºC/min under a nitrogen flow of 100mL/min.

Figure 3.10: A Netzsch model STA 449 F3 Jupiter ® TGA

3.5 Gas permeation measurements:

3.5.1 Pure gas measurement:

The prepared PSF, bare polyamide, and CDCS/polyamide mixed matrix membranes, were examined for pure CO_2 and CH_4 gas permeation. The pure gasses were tested at a feed pressure from (1-5 bar) and at different temperatures (300.15, 308.15 and 323.15 K). The gas permeation experiments were conducted using the well-known constant volume /variable pressure method [32].

As shown in Figure 3.12, the gas permeation apparatus for this method contains a membrane cell module, a specified permeation volume, a vacuum pump that is connected to the permeate volume through a valve, and pressure sensors to detect the feed and permeate pressures. A membrane sample with an area of 4.9087 cm^2 was cut and "fixed inside the membrane cell. The measurement of the gas started by evacuating the system volume and the feed side using the vacuum pump. The gas is then fed into the module at a constant rate. To determine the gas permeability the valve used for the evacuation was closed, which causes the permeate gas to increase slightly with time. The leak rate was measured each time for each single to get accurate permeation rate. The permeability (P) in Gas permeation unit GPU (10^{-6} cm^3 (STP)/sec/cm^2/cm-Hg) was calculated from the following equation (3.1) [28]:

$$P = \frac{273 \times 10^6 \ V_d}{760 \left(P_2 \times \frac{76}{14.7} \right) A \ T} \left[\left(\frac{dP_1}{dt} \right)_{ss} - \left(\frac{dP_1}{dt} \right)_{leak} \right] \qquad (3.1)$$

Where V_d" is the downstream volume (cm^3), A is the effective membrane area (cm^2), P_2

is the upstream pressure (psi), and $\left(\frac{dP_1}{dt}\right)_{ss}$ is the change of the pressure in the downstream chamber at the steady state in $\frac{mmHg}{s}$, $\left(\frac{dP_1}{dt}\right)_{leak}$ is the leak rate in $\frac{mmHg}{s}$ T is the cell temperature in K . The perm-selectivity of gas i to j (αi,j) was estimated by equation (3.2):

$$\alpha i,j = \frac{p_i}{p_j} \qquad (3.2$$

Figure 3.11: The gas permeation apparatus used to test membrane performance

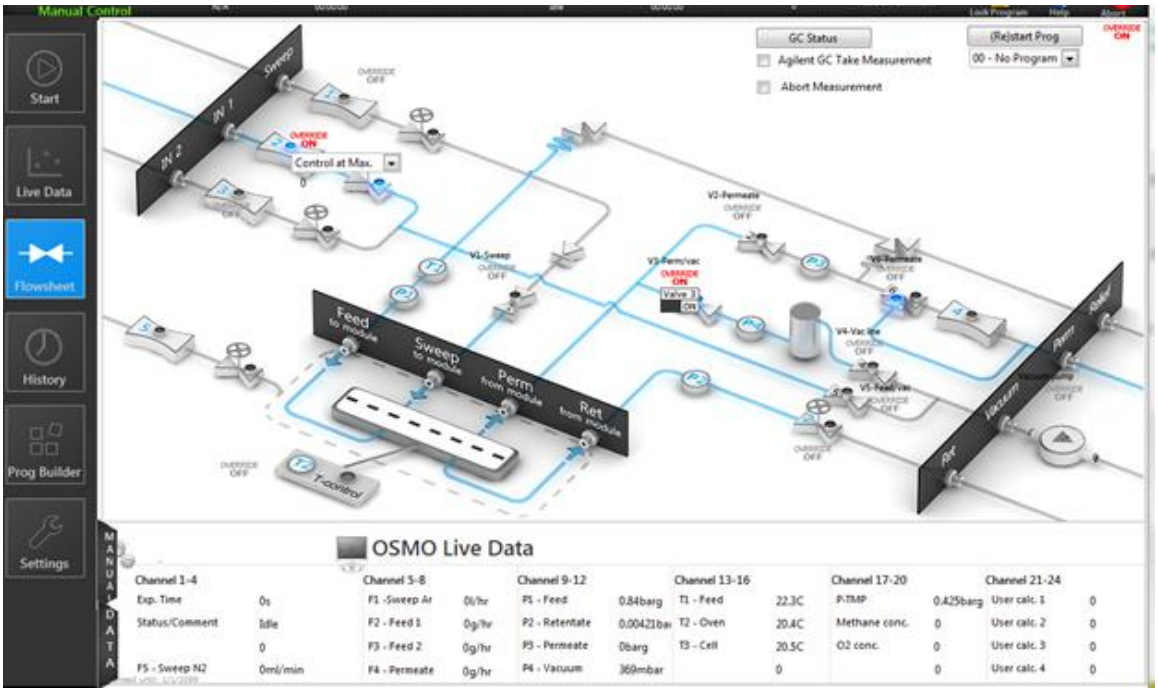

Figure 3.12: Flowsheet of the well-known constant volume/variable pressure method.

CHAPTER 4

RESULTS AND DISCUSSION

4.1 Characterization results:

4.1.1 Membrane Surface Morphology:

In order to confirm the formation of ultra-thin composite polyamide layer on top of PSF support membrane, SEM analysis for both PSF and TFC top surface was carried out. The micrographs SEM images for PSF membranes are shown in Figure 4.1. In which surface morophology of highly porous (Figure 4.1(a)) and dense (Figure 4.1(b)) polysulfone membranes are shown. The porous polysulfone strucutre observed for PSF membranes prepard using convertional wet phase inversion method with DI water coagulation bath. It was observed that PSF membrane has a smooth top surface compared to the rough PA and it has an asymmetric structure with a dense top layer. It is believed that the asymmetric structure resulted from the phase separation along with the instantaneous de-mixing in a quaternary system (polymer, solvent, nonsolvent, and an additive) because DMAC solvent has high mutual affinity for water and the dense layer was built as a result of the dry step before coagulating the membrane in the water bath [31-34]. During the initial step of dry inversion process, THF was removed from the surface of the dope solution because it has the lowest boiling point (65.48 ^{o}C).

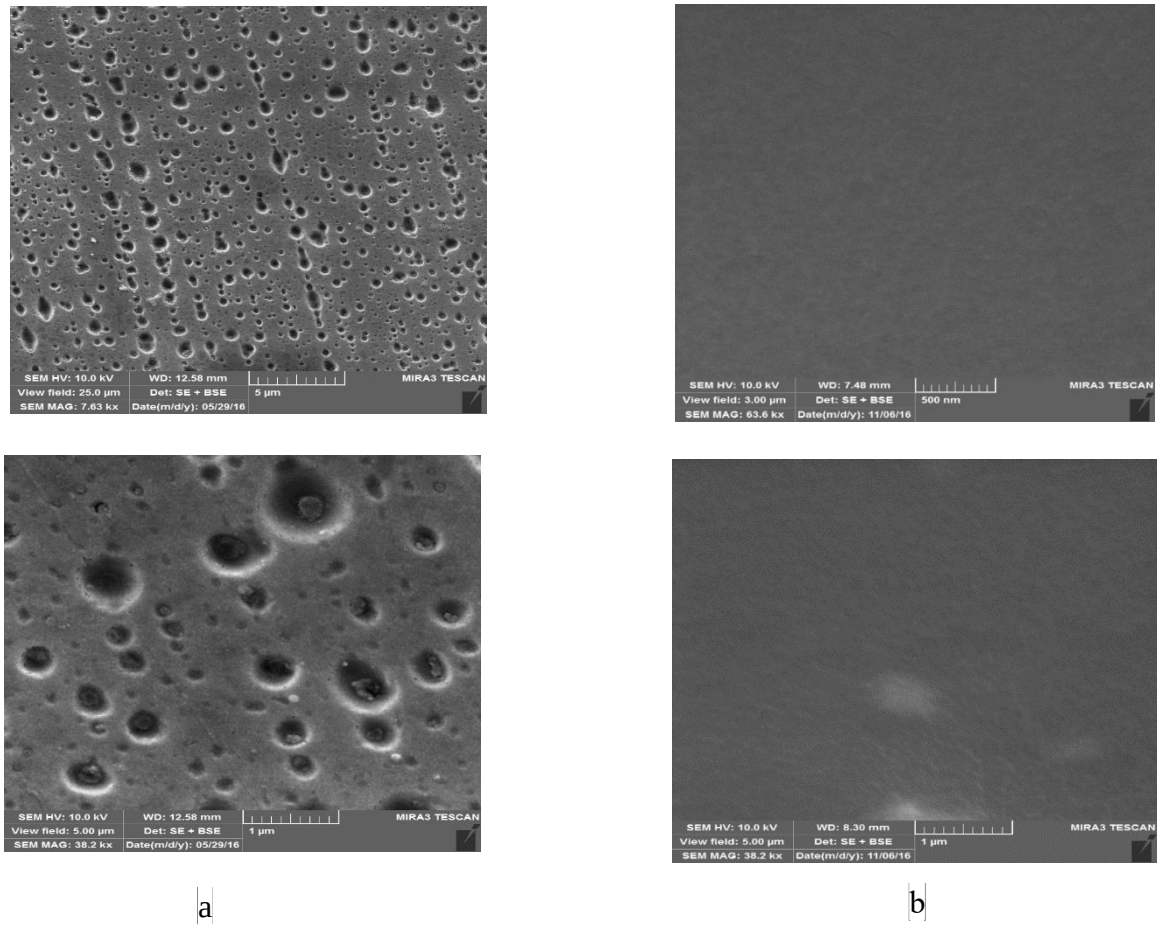

Figure 4.1: Scanning Electron Microscopy (SEM) of: (a) porous PSF, (b) dense PSF membranes

For thin film polyamide surface, SEM images (Figure 4.2 (a)) showed that a defect-free polyamide layer was built on top of PSF layer and the smooth polysulfone surface was totally covered by a rough film of polyamide structure. This layer was formed as a result of interfacial polymerization reaction between PIP and ISC.

Figure 4.2 shows the surface images of pure polyamide and polyamide/CDC nanoparticles mixed matrix membranes prepared using interfacial polymerization method. It can be seen that with increasing nanofiller concentration the structure of skin surface became more rough up to a certain point (loading of 0.5%) then some nanoparticles was agglomerated at

a relatively high concentration of carbide-derived carbon (loading of 1%). In these images, CDC nanoparticles were observed clearly not like other reported images when nanoparticles were not seen on the surface of the membrane.

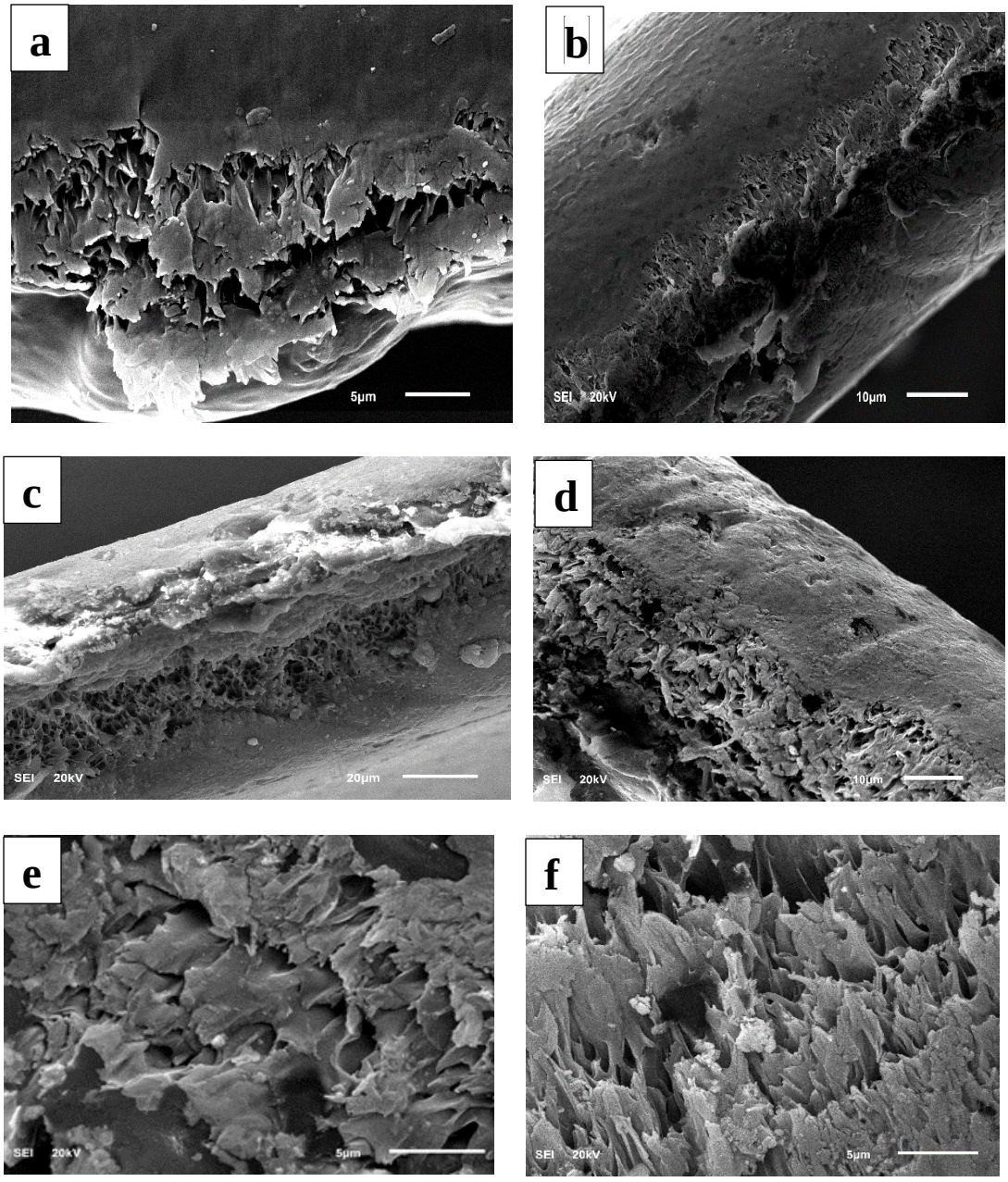

Figure 4.2: Cross section SEM images of:(a) pure PSF (b)Pure polyamide, (c)0.002%CDC/PA, (d) 0.1%CDC/PA, (e) 0.5%CDC/PA, and(f) 1%CDC./PA mixed matrix membranes

(a)

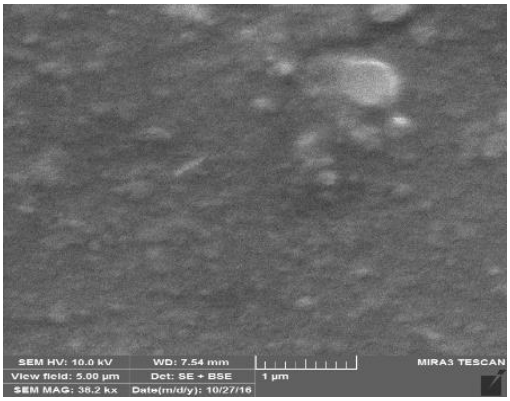

(b)

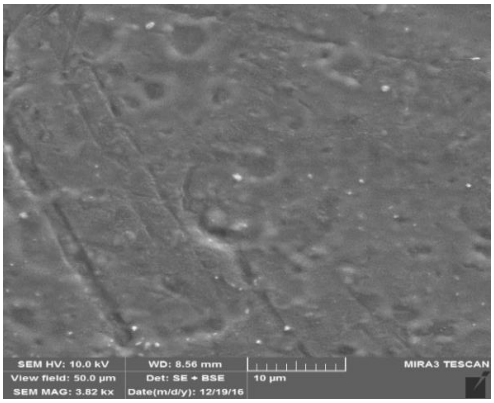

(c)

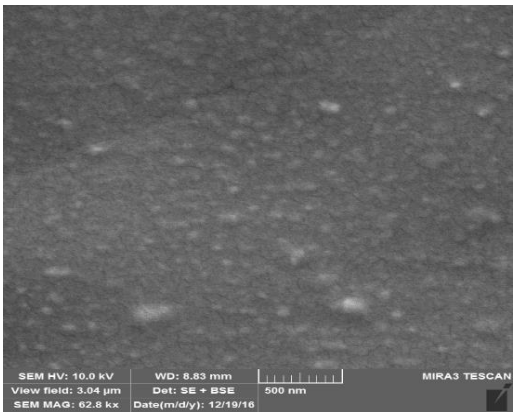

(d)

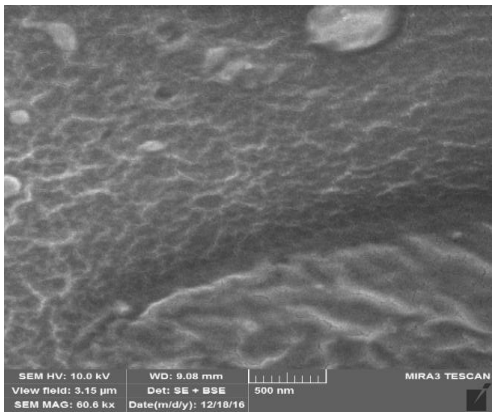

(e)

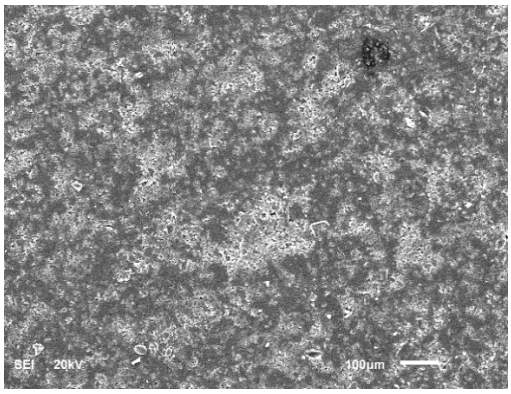

(f)

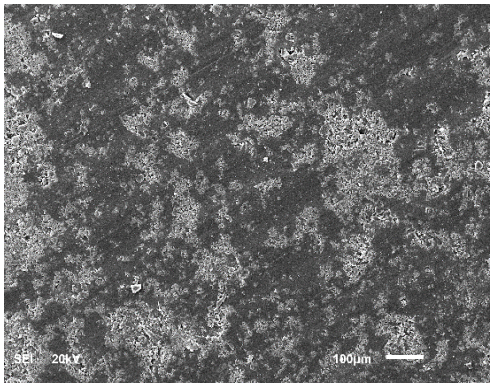

Figure 4.3: surface images of:(a) pure polyamide (b) 0.0005%CDC/PA, (c) 0.002%CDC/PA, (d) 0.1%CDC/PA, (e) 0.5%CDC/PA, and(f) 1%CDC./PA mixed matrix membranes

4.1.2 Fourier transformation infrared (FT-IR):

FT-IR spectra of the entire polyamide–polysulfone composite film, and CDCs/polyamide thin nanocomposite layer were scanned in the range of 400 cm^{-1} to 4000 cm^{-1} to study the chemical composition of the membranes sample. The bands are ascribable for the interfacially polymerized layer as well as PSF support skin because the depth of the beam penetration is thicker than polyamide layer. Figure 4.4 shows the FT-IR spectra of bare Polyamide and CDC/PA MMMs with a CDCs loading of 0.1% and 0.5 %. The band at 1680 cm^{-1} is ascribed to the amide I (C=O) stretch, whereas the broadband at 1590 cm^{-1} is attributed to amide II (C–N) stretch. Moreover, the band of the amine group (NH stretch) was observed at a wavelength of 1500 cm^{-1}. Therefore, the existence of amide I and II in the FT-IR spectra confirmed the formation of the polyamide layer as a result of the IP reaction. The amide bands were observed for CDC/PA membranes and a new peak at 1640 appeared as a result of embedding carbide-derived carbon material to the polyamide film and this peak is ascribed to aromatic carbon bond. We can observed that the characteristic FT-IR peak of CDC nanoparticles at (1600 cm^{-1}) was appeared in CDC/PA MMMs with a small transition. Therefore, FT-IR confirmed the occurrence of IP as well as the successful addition of CDC nanoparticles.

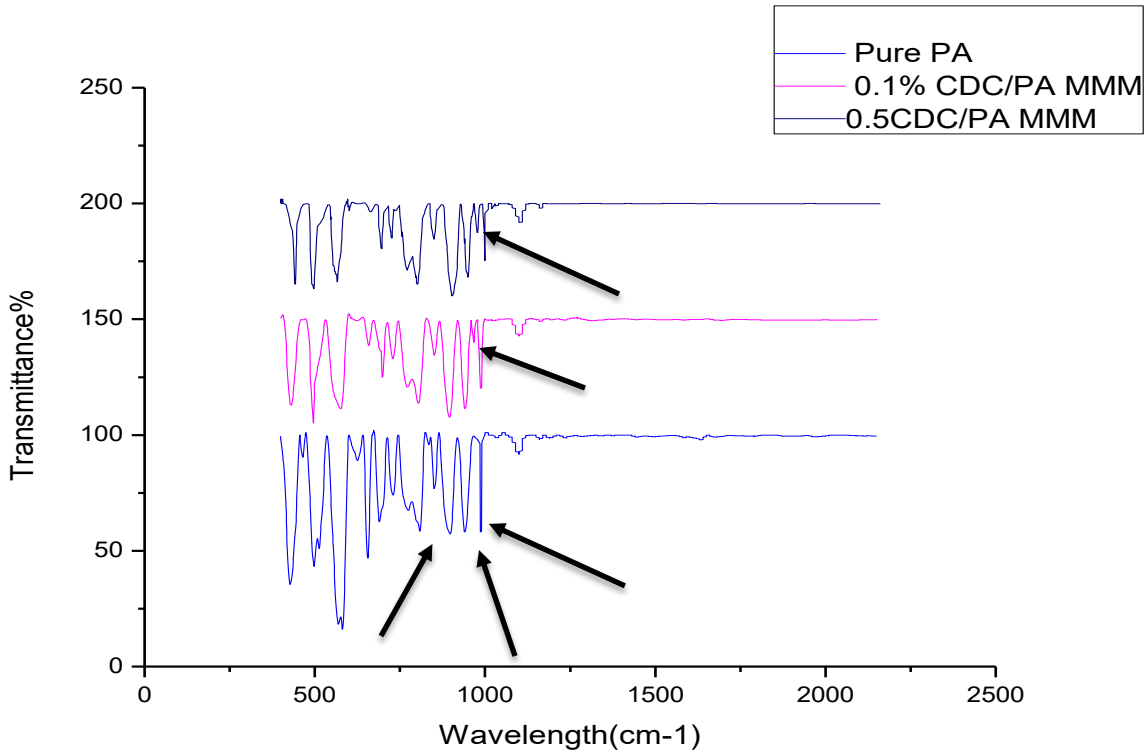

Figure 4.4 FT-IR spectra of Polyamide and CDC/PA MMMs with the loading of 0.1% and 0.5 %

Figure 4.5 reprents FT-IR analysis of Ti-CDC nanoparticles, we can see that CDC nanoparticles have a small peaks at 1600 cm^{-1} which is ascribed to aromatic carbon bond [44] and another peak at 1215 cm^{-1}which is ascribed to the C–N and C–O bonds [45]. The small peak at 3420 cm^{-1} may ascribe to the adsorption of water from the ambient air.

Similar obserevation were reported for Ti-CDC nanoparticles prepared at different temparture (600-120 ºC) [45],[46].

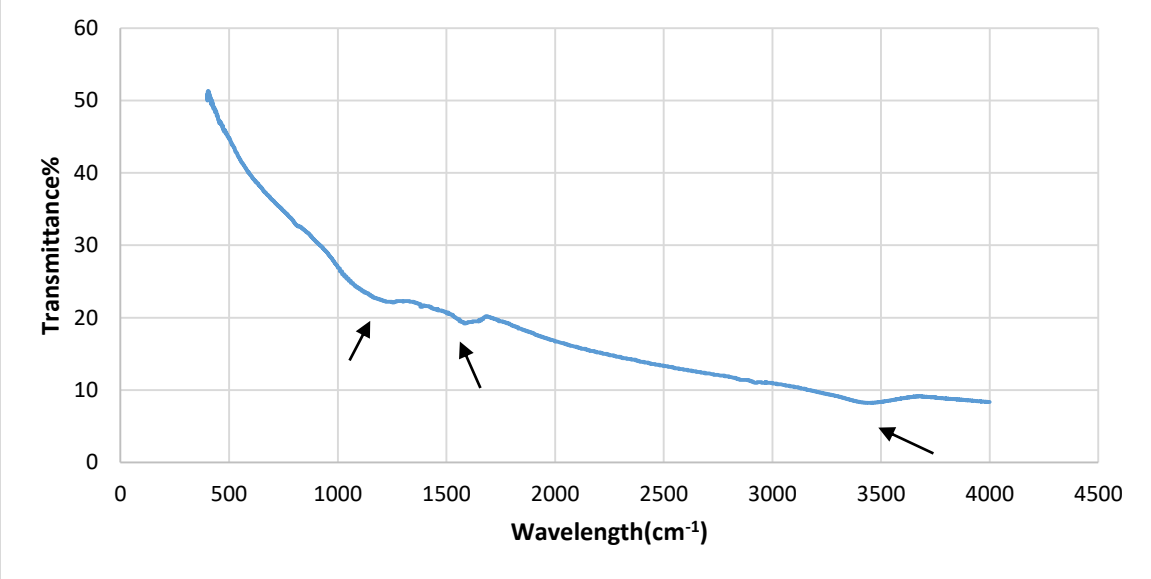

Figure 4.5 FT-IR spectra Ti-CDC nanoparticles

4.1.3 Thermogravimetric analysis (TGA):

The thermal behavior of prepared polyamide membranes, as well as CDCs/polyamide MMMs, were studied by TGA test as shown in the Figure 4.6. Nearly 5-6 mg of samples were heated at a constant heating rate of 10 ºC/min from room temperature to 800 ºC**.** Thermogravimetric analysis of TFC/TFN membranes demonstrated that for all membranes there was no considerable weight loss occurred up to a temperature of 480 °C, which is comparable to the thermal stability of other prepared polyamide reported in the literature[47]. However, pure polyamide membrane started to lose weight significantly at a temperature of approximately 480 °C as the weight reduced from 98% to 33.3% at a temperature of 616 ºC. From Figure 4.6, it is clear that the thermogravimetric curves for TFN have higher residue for all CDCs loading amounts. Which implied better thermal stability of CDCs/PA TFN. Even though all membrane samples of bare polyamide and

MMMs seem to exhibit a similar temperature range (480–620 ^{o}C) for major weight loss, the onset decomposition temperature for bare polyamide membrane was lower than the onset temperature for membranes with CDCs nanoparticles. Generally speaking, inorganic fillers have good thermal strength in comparison to the polymeric material. Upon heating, carbide-derived carbon materials absorbed the heat, and consequently suppressed the rate of membranes decomposition which resulted in relatively higher decomposition temperature [48]. Furthermore, the residue of CDCs/PA membranes at the end of the thermal cycle were 36.66% and 38.32% for 0.1% CDC/PA and 0.5% CDCs /PA MMMs; respectively. Which are higher than the residue of bare polyamide (30.345 %). Therefore, embedding CDC nanoparticles into polyamide matrix enhanced the thermal strength of the membranes. The thermal stability could be evaluated better in terms of $T_{d50\%}$, and $T_{d60\%}$, values (the temperatures at which the tested membrane loses 50, and 60 of its initial mass; respectively. The TGA data showed that the value of $T_{d50\%}$, and $T_{d60\%}$ for bare polyamide occurred at a temperature of 534°C, and 546 °C; respectively, while for the mixed matrix membranes $T_{d50\%}$, and $T_{d60\%}$ occurred in the range (543-546°C), and (574-586°C); respectively.

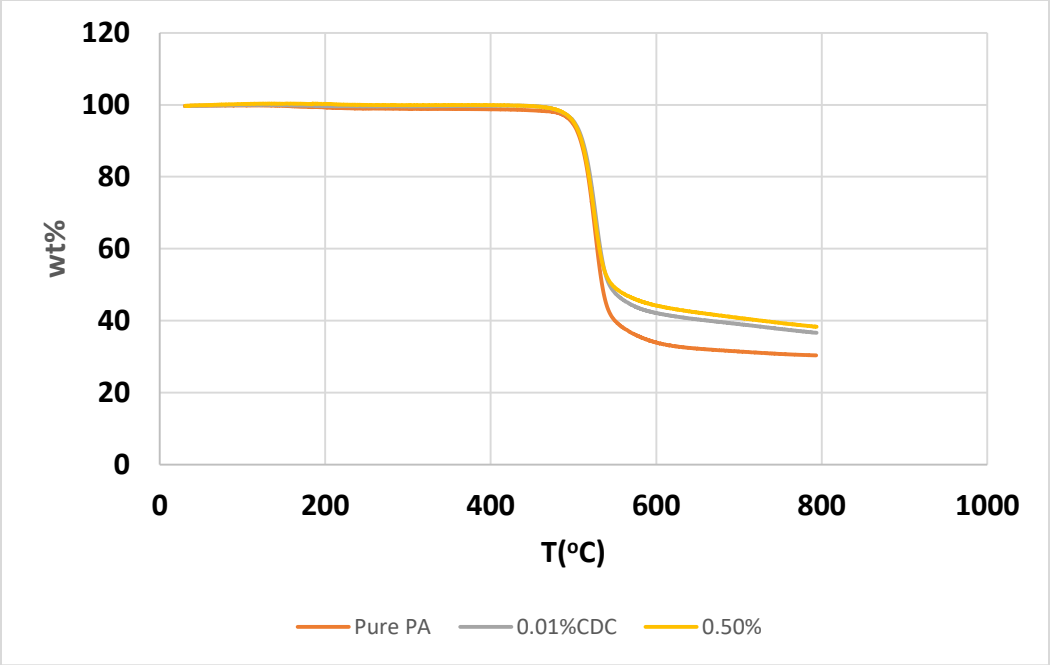

Figure 4.6: TGA analysis for polyamide membranes and CDCs/polyamide MMMs with different nanoparticles loading.

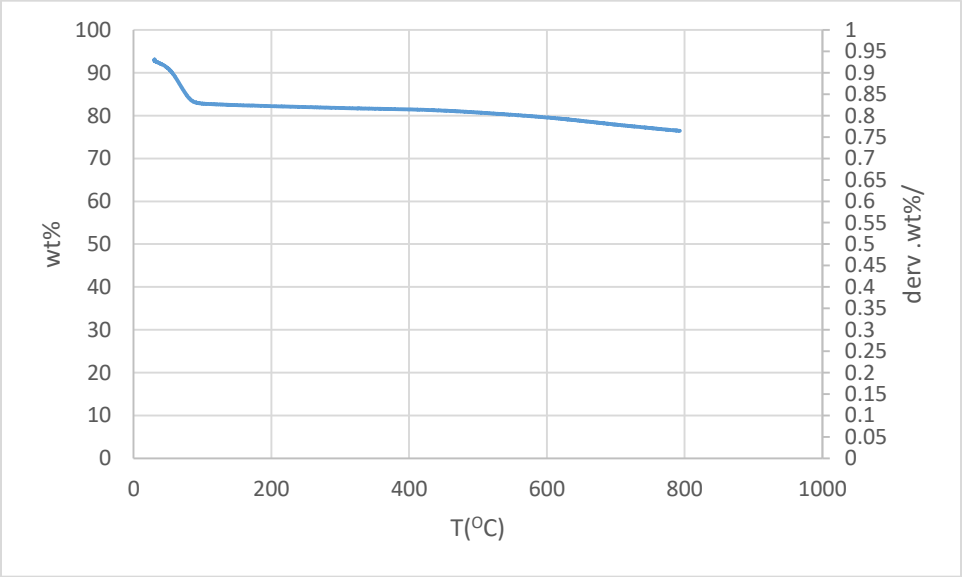

Figure 4.7 TGA analysis of CDC nanoparticles

The TGA analysis of CDC nanoparticles is shown in Figure 4.7, where we can see that CDCs nanoparticles experienced major weight loss in the temperature range of (51-90 ^{o}C) and the weight at the end of the cycle was 76.45%.

4.1.4 X-ray diffraction (XRD):

Bruker D8-Advance X-ray diffractometer was used to take XRD spectra of, bare polyamide, and Ti-CDC/PA MMM with a wavelength of 1.5414 Å. The angle of diffraction (2Θ) was changed from 5^{o} to 50^{o} in order to observe the nature of the membrane structures. A scanning rate of 2^{o}/min operating at 30kV and 30mA was used for XRD spectra. Figure 4.8 shows the microstructure of Ti-CDCs, polyamide, and CDC/PA MMMs. It can be seen that for carbide derived carbon there are two peaks at angle (2Θ) of 26^{0} and 43^{o}. The peak at 26^{0} is attributed to (002) planes of graphite while the peak at 43^{o} corrosponds to diffraction from (101) planes of graphite. These peaks implied the crystialline strucure of the prepared Ti-CDC. Similar finding were reported in literature for Ti-CDC prepared at 800 ^{o}C [49],[50].The structure of CDC nanoparticles depends on the preparation condition. Generally speaking, amorphous CDCs can be prepared at low temperature while treating Ti metal at high temperature produces crystalline Ti-CDC nanoparticles. As shown in the XRD spectra of PA membrane, the broad peak centered around 19° revealed the amorphous structure [51]. While the very small peak around 21° indicates the semi-crystalline nature of composite thin layer. The presence of crystalline regions can be attributed to the thin polyamide layer, while amorphous regions appeared as results of PSF structure [15]. The XRD patterns of Ti-CDCs /PA nanocomposite membranes with different loading were almost identical to that of the bare polyamide

membrane. Therefore, the addition of CDC nanoparticles did not change the crystallinity of pure polyamide membrane.

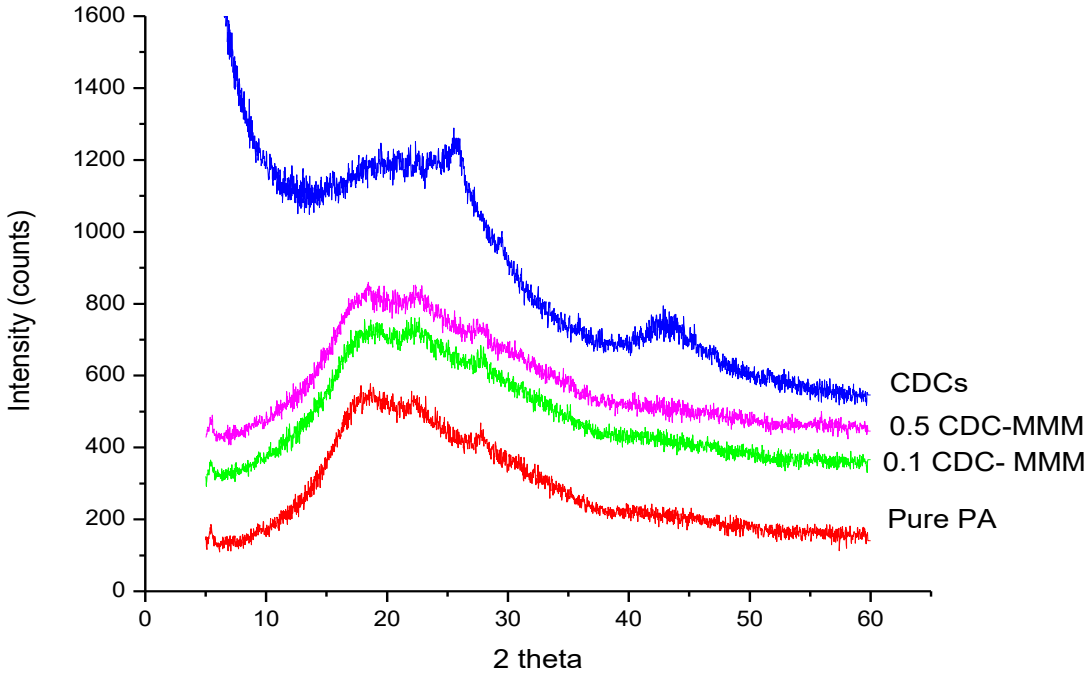

Figure 4.8: XRD pattern of CDC nanoparticles, composite polyamide, and carbide-derived carbon, and PA/CDC mixed matrix membrane

4.2 Gas permeation measurement:

4.2.1 pure gas permeability and selectivity:

Gas separation performance of the fabricated polysulfone support, thin film polyamide membranes, as well as carbide-derived carbon (CDC)/polyamide mixed matrix membranes, were evaluated using pure gas of carbon dioxide (CO_2), and methane (CH_4) at different temperatures (from 300.15 to 323.15 K) and at a feed pressure from (1-5 bar). It is known that amide and free amine groups in the polyamide membrane render the

facilitated transport mechanism of CO_2 and these functional groups are activated in presence of moisture in the membrane [40,24]. Therefore, our membrane samples were saturated by DI water before testing the gases to benefit from the facilitated transport mechanism of CO_2. Table 4.1 represents the separation performance of polysulfone, polyamide, and CDC/PA MMMs at a temperature of 300.15 K and pressure of 5 bars. Overall experimental results revealed that membranes with CDC nanoparticles experienced higher permeance and selectivity than pure polyamide thin film membrane. Moreover, polyamide membrane showed higher perm-selectivity than polysulfone support. From Table 4.1, we can observe that building polyamide thin film layer on top of PSF membrane increased the gas selectivity while the gas permeability decreased as a result of the increased mass transfer resistance. CO_2 was found to be the fastest moving gas molecule for all type of membrane samples tested in these experiments with a permeance of 2.16 and 2.41 GPU for polyamide and polysulfone membranes, respectively. Whereas, CH_4 was the lowest moving gas molecule with a permeance of 0.162 and 0.556 GPU for polyamide and polysulfone membranes at the exact same conditions. From table 4.2, we can see that incorporation of carbide-derived carbon into polyamide film layer enhanced the permeance of both CO_2 gas molecules and CH_4 gas. The enhancement in gas molecules permeation was primarily attributed to the addition of carbide-derived carbon nanoparticles which offered faster gas flow. As confirmed by SEM images in Figure 4.2 CDC nanoparticles dispersed well in polyamide thin film. Which resulted in higher gas permeance since the well-dispersed CDCs could serve as channels to transport gas molecules more effectively. Furthermore, the average pore size of the used CDCs is 1.542 nm (15.42 A˚) which is considerably larger than kinetic diameters of CO_2 (3.30A˚) and

CH_4 (3.8A˚) molecules. Moreover, the superior characteristic properties of CDCs in term of high surface area offered more surface and volume for gases to diffuse and absorb into the membrane matrix. Similar findings were observed in the literature [37, 38, 44] for using carbon materials as inorganic fillers. Generally speaking, incorporation of carbon materials disrupt the polymer matrix chain and improve the gas diffusion as a result of the higher free volumes. From Table 4.1, by embedding CDC nanoparticles with a loading of 0.5%, CO_2 permeance enhanced from 2.16 to 4.07 GPU, while CH_4 increased from 0.162 to 0.204 GPU. Clearly, CO_2 enhancement is much higher that CH_4 which resulted in higher CO_2/CH_4 selectivity at a value of 19.92. As a whole, the gas permeation of the prepared thin film composite polyamide membrane, PSF membrane, and CDC/PA MMMs followed the order of kinetic diameters of gas molecules tested in the experiments. Since the order of gas permeance was $CO_2 > CH_4$ and the kinetic diameters of gas molecules are 0.330 nm for CO_2, and 0.380 nm for CH_4. Since CO_2 is a soluble gas, It is believed that CO_2 gas undergoes dissolution in the polyamide film layer which contains polar –NHCO functional groups [53]. Moreover, CO_2 molecules are expected to form hydrogen bonding interactions with amide groups from the polyamide membrane. On the other hand, CH_4 is relatively saturated non-polar molecules that exhibited very low interaction with the membrane and showed very low permeabilities. As we mentioned before, , in the wet condition of the membrane, a reversible reaction between amine groups and CO_2 molecules is expected to occur which produces complex and HCO3 – components that could diffuse freely through the membrane based on solution–diffusion mechanism [54].. Furthermore, CH_4 molecules transport through the membrane based on simple solution–diffusion mechanism. As a result of the high permeance of CO_2 comparing to CH_4, relativity high selectivities of CO_2/

CH_4 $_2$ gas pair was recorded for the fabricated TFC membranes at a value of 13.33 for pure polyamide and 19.92 for CDC/PA MMMs at 0.5% CDC loading.

Table 4.1: separation performance of polyamide membrane, polysulfone support and CDC/PA MMMs at a temperature of 300.15 K and pressure of 5 bars

Membrane	Loading %	CO_2	CH_4	CO_2/CH_4
PSF	0	2.41	0.556	4.33
PA	0	2.16	0.162	13.33
MMM1	0.0005	2.33	0.163	14.36
MMM2	0.002	2.44	0.169	14.51
MMM3	0.1	3.13	0.186	16.86
MMM4	0.5	4.07	0.204	19.92
MMM5	1	5.00	0.375	13.31

4.2.2 The effect of nanoparticles loading:

In order to investigate the effect of CDCs nanoparticles loading on the separation performance of the fabricated TFN membranes, CDCs/Polyamide MMMs with different CDC nanoparticles loadings were prepared and compared with neat thin film composite polyamide membrane for separation of CO_2/CH_4. Figure 4.9 and 4.10 show the change in CO_2 and CH_4 gas permeance with varying CDCs loading from 0.0005 % to 1%. Different mixed matrix membranes with different CDC loadings were prepared as follow: MMM_1, MMM_2, MMM_3, MMM_4 and MMM_5 for 0.0005%, 0.002%, 0.1%, 0.5% and 1% CDCs loading respectively. It is obvious that the permeation rate of both CO_2 and CH_4 gas molecules enhanced with increasing the loading of CDCs nanoparticles in polyamide composite layer. Which can be attributed to the good interaction between polyamide matrix and nanofiller surface. In addition to, the good adhesion of CDC in polyamide chain.

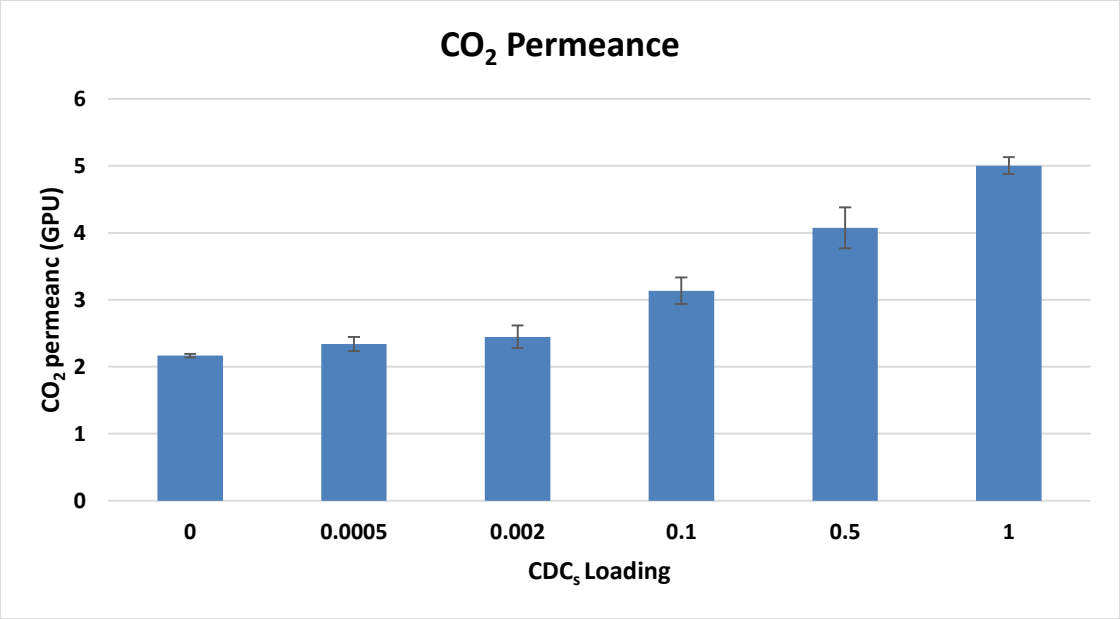

Figure 4.9: The effect of CDCs nanoparticles loading on CO_2 permeance.

Even though both CO_2 and CH_4 gas permeation increased with increasing CDC loading, the increments were not the same for the two gasses. From Figure 4.9, CO_2 permeance initially increased from 2.16 GPU for pure polyamide to 2.33 GPU for MMM_1 with 0.0005% CDC loading, and continued to increase to 2.44 GPU for 0.002%. The permeance of CO_2 gas for $MMM_3$with 0.1% loading was 3.13 GPU and it enhanced to 4.07 GPU for 0.5 % loading and the maximum amount of CO_2 permeance was recorded at 1% loading with a value of 5.00 GPU. While from Figure 4.10, CH_4 gas molecules permeation increased from 0.162 GPU for the neat PA to 0.169 GPU for MMM_2 at 0.002% loading. Moreover, 0.186 and 0.204GPU were recorded for 0.1 % and 0.5 % CDC loadings respectively and 0.375 GPU was the maximum value of CH_4 permeance observed at 1 % nanoparticles loading. The much higher increase in CO_2 permeation comparing to CH_4 was responsible for the improvement in CO_2/ CH_4 selectivity.

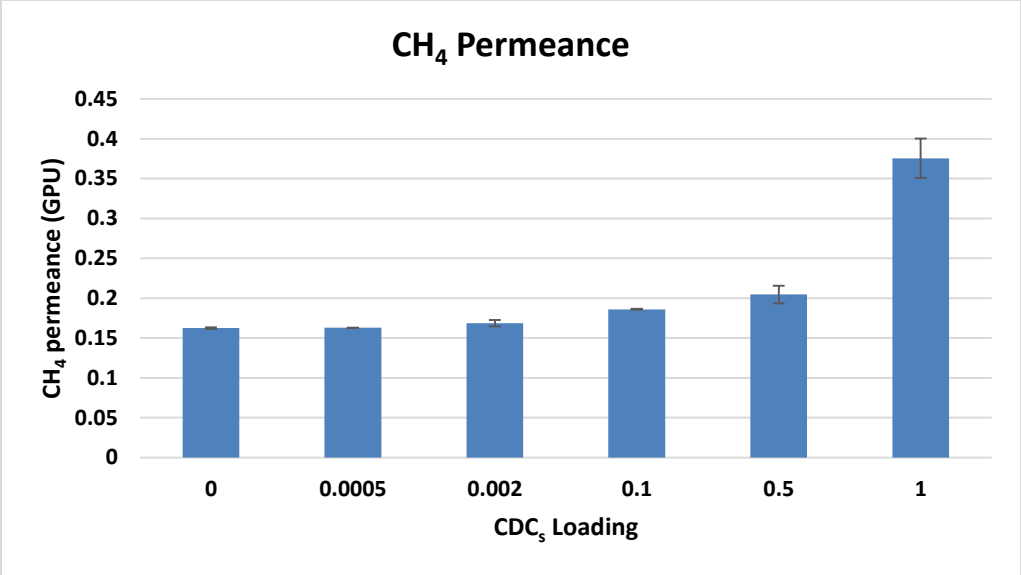

Figure 4.10: The effect of CDCs nanoparticles loading on CH_4 permeance.

From Figure 4.11, It can be seen that the CO_2/CH_4 gas pair selectivity of pure thin film polyamide membrane was improved by incorporating CDC nanoparticle into polyamide matrix with a loading of 0.0005% (MMM_1), and the selectivity continued to increase with increasing the loading up to 0.5 % CDC loading then CO_2/CH_4gas selectivity decreased to 13.31. The reason behind the deterioration in the selectivity was attributed to the increment in the free volume that resulted in a much higher increase in CH_4 permeance in comparison with CO_2 permeance because CH_4 has higher kinetic diameter. As shown in Figure 4.9 and 4.10, when CDC loading increased from 0.5% to 1%, CO_2 enhanced by 22.8% while CH_4 permeance increase was 83.82%. Which resulted in deterioration of the selectively to a value of 13.31. The much higher increase in CH_4 permeance compared to CO_2 permeance could indicate the creation of defects in the membrane surface, thereby more CH_4 gas molecules permeate because it has higher kinetic diameter (0.38nm). Moreover, CDCs agglomeration that observed in SEM images in Figure 4.2 for 1% loading might be responsible for the deterioration in the gas selectivity.

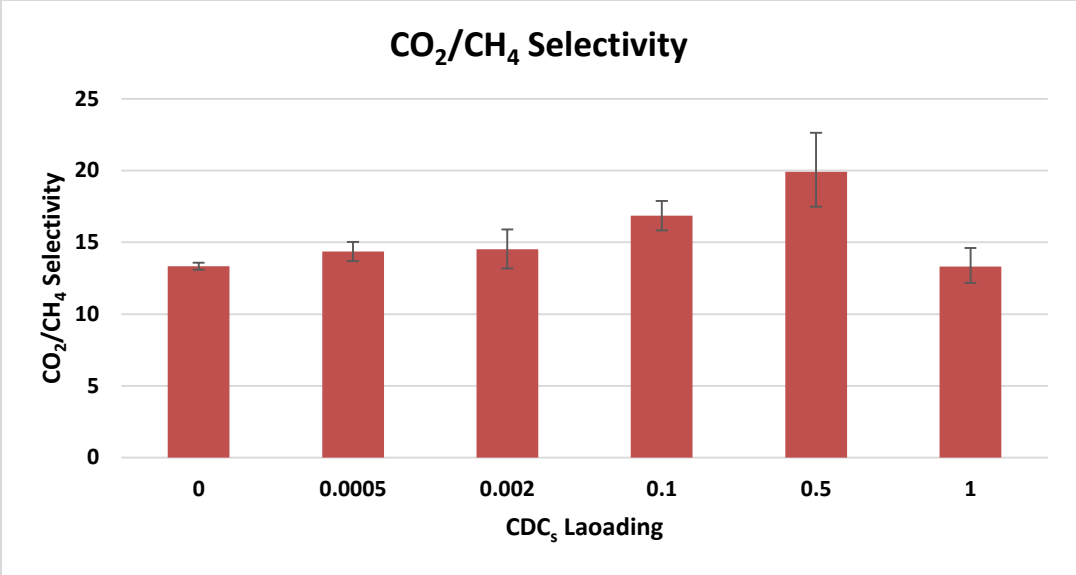

Figure 4.11: The effect of CDCs nanoparticles loading on CO_2/CH_4 Selectivity.

4.2.3 The effect of the number of layers:

In order to study the effect of the number of selective polyamide layers on the separation performance of CO_2/CH_4 gas pair, CDC/polyamide mixed matrix membrane with the best loading amount of 0.5 % prepared with different number of layers as follow M_1 (1 layer), M_2(2 layers), M_3(6 layers), and M_4 (10 layers) of selective CDC /PA layer. Figure 4.12 shows the permeability of CO_2 and CH_4 gas molecules as a function of the number of selective nanocomposite layers.

CO_2 as well as CH_4 gas permeance, were reduced as the number of layers increased because of the higher membrane thickness which offered higher resistance for the gas permeation. From Figure 4.12, CO_2 permeance reduced from 4.07 GPU for 1 layer to 3.36, 3.33, and 2.32 GPU for 2, 6, and 10 layers respectively. While from figure 4.13, we can observe that

CH_4 permeation decreased from 0..204 GPU for 1 layers to 0.167, 0.144 and 0.096 GPU for 2, 6, and 10 selective layers.

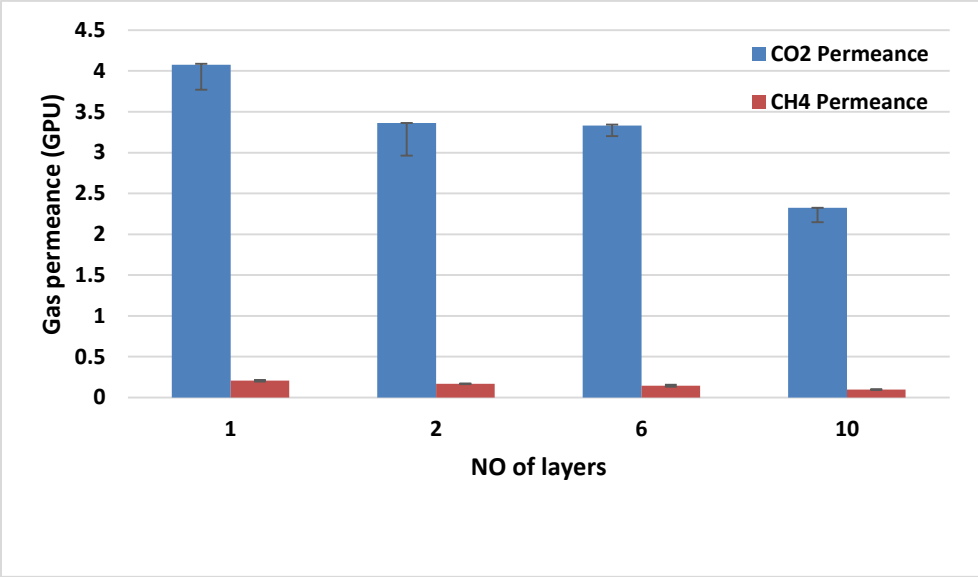

Figure 4.12: The effect of the number of layers on gas permeance.

The reduction in the gas permeance was accompanied with much enhancement in CO_2/CH_4 selectivity as shown in Figure 4.13, wherein the selectivity improved from 19.91 for I layer membrane to 20.9, 23.19, and 24.08 for 2, 6, and 10 numbers of layers. The higher selectivity of CO_2/CH_4 was attributed to the functional group of the CDC /polyamide which offered higher permeation of CO_2 than CH_4.

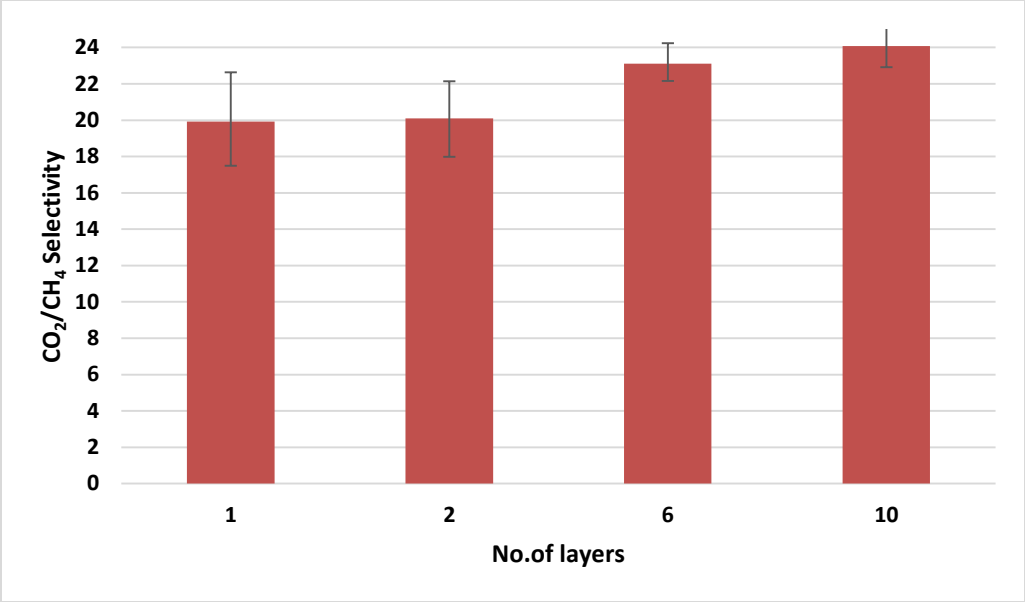

Figure 4.13: The effect of the number of layers on CO_2/CH_4 permeance.

4.2.4 The effect of operating temperature on the separation performance:

Polysulfone, TFC polyamide, as well as CDC/polyamide membranes were subjected to a temperature varying from 300.15 to 323.15 K using two pure (CO_2, and CH_4) gasses in order to study the effect of temperature on the membrane separation performance. The gas permeance and gas selectivity values of different gasses through the TFC, TFN, and PSF membranes at different temperatures are given in Table 4.2. The temperature dependence of gas permeability could be expressed by the Arrhenius equation as follow:

$$P = P_0 \, Exp(\frac{-E}{RT}) \qquad (4.1)$$

Table 4.2: The effect of operating temperature on the separation performance of polysulfone, polyamide, and CDC/PA mixed matrix membranes at 5 bar.

Polysulfone				Polyamide			CDC/polyamide		
T(k)	CO2	CH4	CO2/CH4	CO2	CH4	CO2/CH4	CO2	CH4	CO2/CH4
300.15	2.41	0.556	4.33	2.12	0.175	12.08	4.07	0.204	19.92
308.15	2.45	0.605	4.05	2.44	0.221	10.75	4.14	0.254	16.26
323.15	2.85	0.840	3.38	2.80	0.301	9.29	4.89	0.319	15.32

Generally speaking, for polymeric membranes, increasing the operating temperature results in higher free volume for gas molecules to transport and more flexible polymer chains. Which leads to enhanced both gas diffusion and permeation. At the same time, lower pair gas selectivity is expected by increasing the temperature as a result of the wider polymer chain motions and more loose structure of the membrane. From Table 4.2, one can see that all gas molecules permeation enhanced with increasing the operating temperature. Nevertheless, the permeation increase was not the same for all gasses from one gas to another, for instance, by raising the temperature of polyamide membrane from 300.15 to 323.15 K, CO_2 permeance increased by 31.13 % while, at the same temperature range for CH_4 gas molecules there was an enhancement of the permeation by 72.0% from. The reason beyond the much higher increase in the permeance of CH_4 is that the permeation of this gas is based on simple molecules diffusion while CO_2 gas has a strong interaction with functional groups of the polyamide membrane which results in higher solubility and lower diffusivity. This solubility is reduced with increasing temperature and the reduction is higher for the more condensable gas (CO_2) in comparison with CH_4 gas molecules.

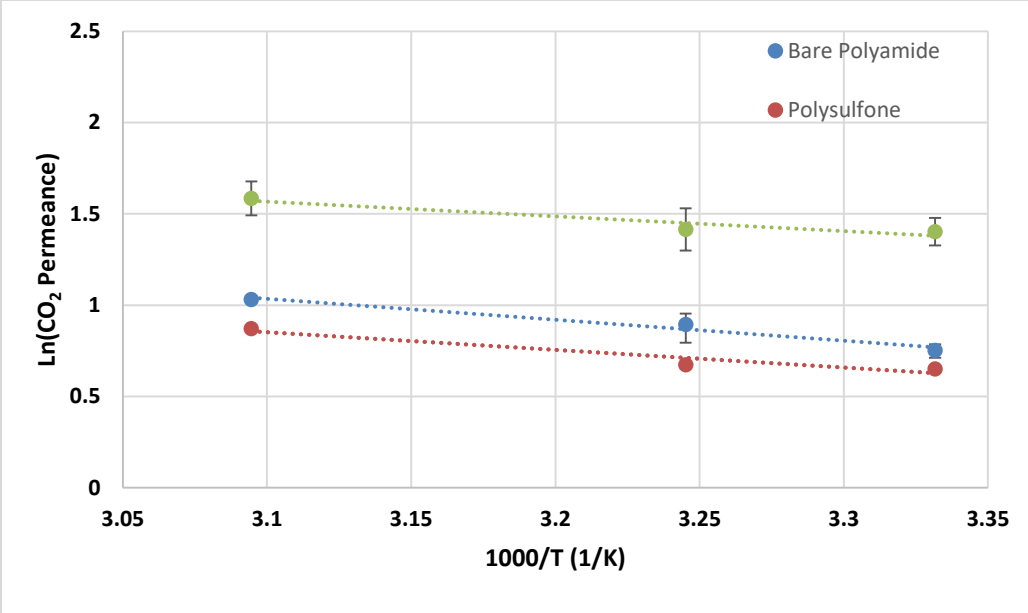

Figure 4.14: linear decrease of the logarithm CO_2 gas permeation with raising the reciprocal temperature

Figure 4.14 shows the linear decrease of the logarithm gas permeation with raising the reciprocal temperature. Ln P was plotted against 1/T in order to calculate the activation energies for permeation of CO_2 and CH_4 gas for polyamide, PSF support, and CDC/PA membranes. lnP (CO_2) vs.1/T representative plot is shown in Figure 4.15 and the values of the activation energies of CO_2, and CH_4 for TFC, PSF membranes, and MMM are tabulated in Table 4.3.

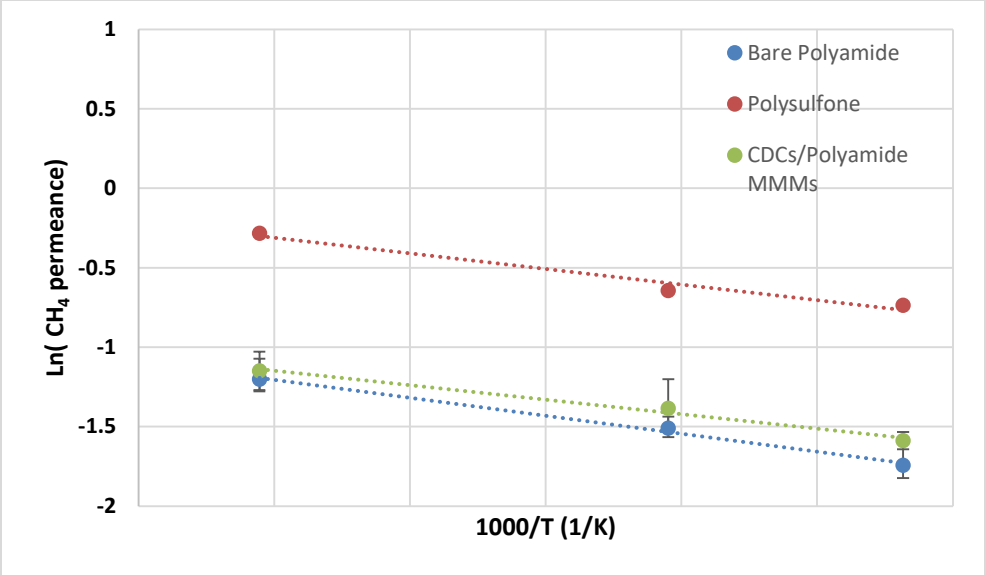

Figure 4.15: linear decrease of the logarithm CH_4 gas permeation with raising the reciprocal temperature

The permeation activation energies followed the gas permeability of the gas molecules and they were in the following order$E(\mathrm{CO2}) < E(CH4)$. Susanta et al [61,62,63], reported similar observation for polyimide, polyarylene ether, cellulose membranes. They attributed the low activation energy of the CO_2 to the high solubility in the polyamide backbone [64,48]. From literature, E is affected by the gas and polymer interaction as well as the molecular size of penetrant [31]. Generally, gases with lower activation energies moves faster through the membrane and vice versa. The solution-diffusing mechanism suggests that E of gases contains two contributors: $E_d$which is usually positive and ΔH_s (Eq. (4.2)). Condensable gases, such as CO_2 have large negative ΔH_s that results in significant reduction of the solubility with increasing the temperature. In contrary, for non-interacting gasses (like CH_4,) $\Delta H_{Condensation}$ is negligible and ΔH_{Mix} is dominant. Hence, for theses gas molecules the solubility reduces slightly with raising the operation temperature [20].

Table 4.3: Activation energies of (CO_2 and CH_4) for polyamide and polysulfone membranes (kJ/mole).

Membrane	E_{CO2} (kJ/mole)	E_{CH4} (kJ/mole)
Polysulfone	8.04	16.32
Polyamide	9.53	18.77
CDC/PA MMM	6.74	15.27

The trend of the selectivity values for the pair's gas with increasing temperature for polysulfone support, polyamide, and CDC/Polyamide membranes are shown in Figure 4.16. The increment in the permeation of CH_4 gas with high E was higher than the increment of CO_2 permeace as the temperature increased. Therefore, CO_2/ CH_4, pair gas selectivity decreased with increasing the temperature.

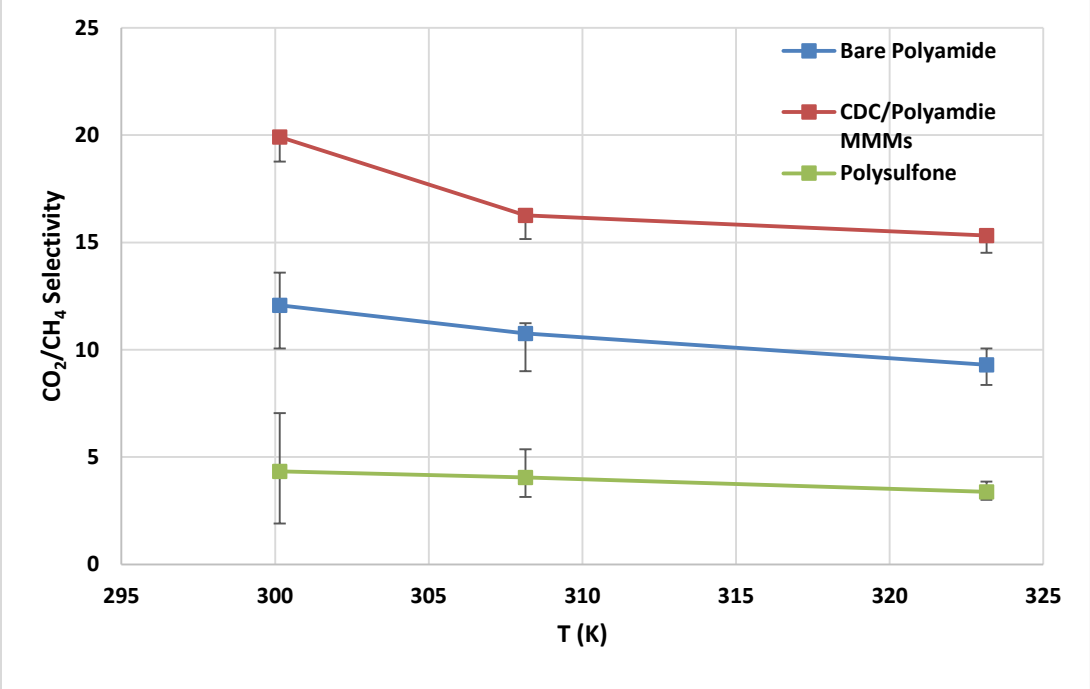

Figure 4.16: The effect of operating temperature on CO_2/CH_4 selectivity

4.2.5 The effect of feed pressure on the separation performance:

To investigate the effect of the gas feed pressure on the separation performance of the fabricated polysulfone, neat polyamide and thin film nanocomposite CDC/polyamide membranes, different feed pressures were subjected to the membranes at a constant temperature of 300.15 K and the results are illustrated in Figure 4.17 and Figure 4.18. It can be seen that CO_2 permeance for both polyamide and CDC/Polyamide membranes decreased with increasing gas feed pressure, while for polysulfone membrane there was a slight increase in that CO_2 permeance. While in Figure 4.18 CH_4 permeance increased quite slightly. For polyamide membrane it is known that the CO2 reacts with the polyamide membrane (according to Eq.1.3) to produce a complex and HCO3– which can diffuse from one site to another. Therefore, by increasing the CO2 amount within the membrane, amine carriers might reach the saturation state and cannot combine with other CO2 molecules anymore, thereby lower CO2 permeance is expected from this mechanism of CO2 permeation. Whereas, for polysulfone, the enhanced CO_2 permeance can be attributed to the higher molecular concentration of CO_2 at the gas membrane interface, which results in better gas and polymer chains interaction.

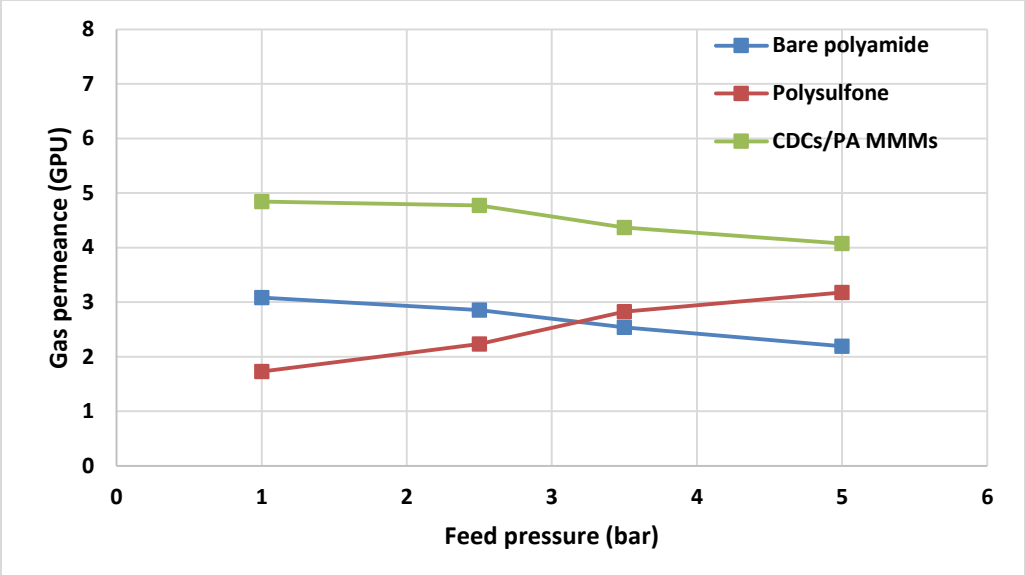

Figure 4.17: The effect of feed pressure on CO_2 permeance for PSF, polyamide, and CDC/PA mixed matrix membranes.

Another possible explanation for the decrease in CO_2 permeance is that according to the dual mode sorption model (DSM) which is common for glassy polymer [58]. At higher feed pressure polymer chains get more compact which results in lower fractional free volume (FFV) of polymer and consequently, the gasses diffusivity declines. From Figure 4.17 we can see that for pure polyamide membrane CO_2 permeance decreased from 3.084 to 2.16 GPU when the feed pressure increased from 1 to 5 bar, and the decline in CO_2 permeance for CDC/Polyamide membrane was lower as the permeance decreased 4.82 from to 4.07 GPU for the same range of pressure increase and that is because carbide-derived carbon nanoparticles provided more free volume for gas to move and therefore higher diffusion is expected. Whereas, CO_2 permeance for polysulfone membrane improved from 1.72 to 3.17 GPU for the same range of the pressure increase

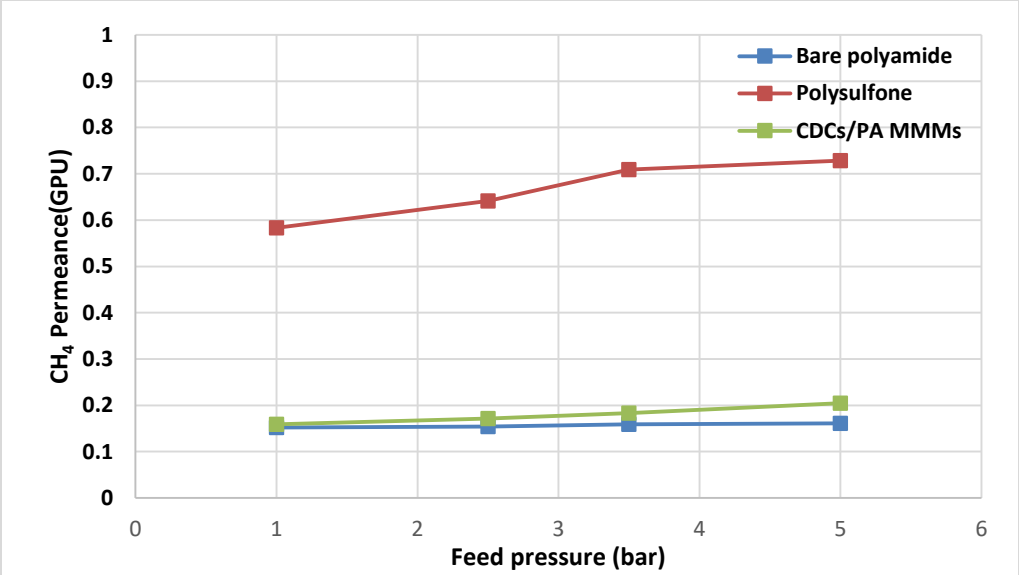

Figure 4.18: The effect of feed pressure on CH_4permeance for PSF, polyamide, and CDC/PA mixed matrix membranes

CH_4 permeance for polyamide membrane was almost constant when the feed pressure increased from 1 to 5 bar. Because CH_4 molecules did not react with polyamide membrane, the transport of methane gas across the membrane is based on simple solution–diffusion mechanism. As a result of the decreased CO_2 permeance with raising gas feed pressure CO_2/CH_4 gas selectivity reduced. According to the dual mode sorption model which is common for glassy polymer [30,45]. At high feed pressure polymer chains get more compact which results in lower fractional free volume of polymer and consequently, the gas diffusivity declines. This phenomena could be another reason for the decrease in CO_2 permeance. From Figure 4.18 we can see that when the feed pressure increased from 1 to

5 bar, CO2 permeance for polyamide membrane decreased from 2.97 to 2.12 GPU.

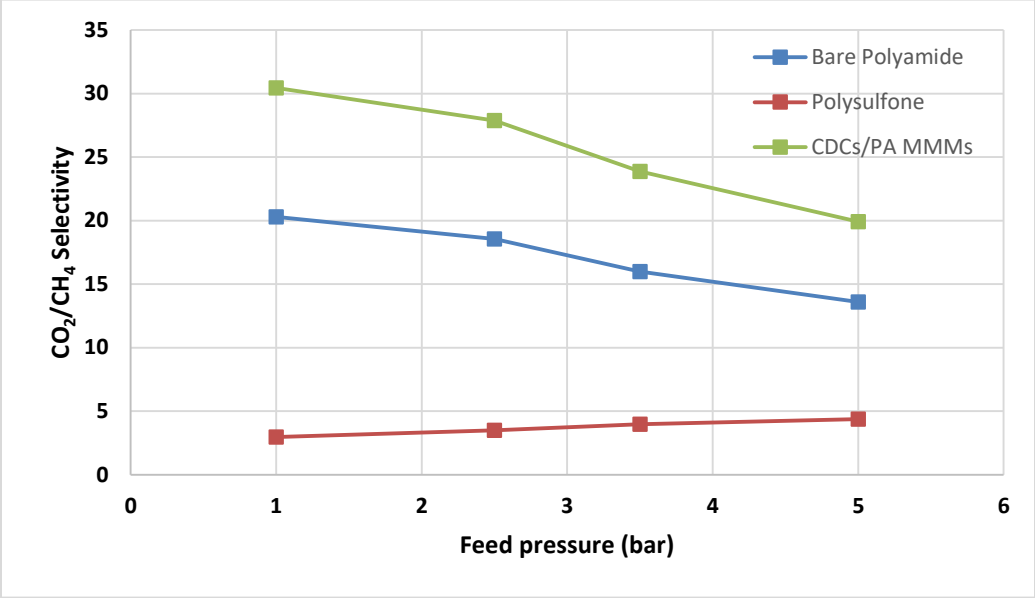

Figure 4.19: The effect of feed pressure on CO_2/CH_4 selectivity for PSF, polyamide, and CDC/PA mixed matrix membranes

Figure 4.19 illustrates the effect of increasing feed pressure on CO_2/CH_4 selectivity. As we can see gas selectivity of both polyamide and CDC/polyamide membrane decreased with increasing the feed pressure as a result of the reduction in CO_2 permeance while CH_4 permeance remained almost the same (unnoticed increase). Whereas, for polysulfone membrane, there was insignificant increase in the gas selectivity caused by the increased solubility of CO_2 as compared to CH_4 molecules.

CHAPTER 5

CONCULSIONS AND RECOMMONDATIONS

5.1 Conclusion:

The uniqueness of this research has been the successful use of titanium carbide-derived carbon as a nanofiller to fabricate mixed matrix membrane. The conclusion of this study can be summarized as the following:

- Defect-free polysulfone, polyamide, and thin film CDCs/polyamide membranes were successfully fabricated and characterized for the morphologies, chemical composition, thermal stability, and crystallinity.
- Gas permeation measurements showed that polyamide membrane had higher CO_2/CH_4 selectivity (178%) compared to polysulfone membrane and this enhancement in the selectivity was attributed to the presence functional groups (amine groups) in polyamide layer.
- Incorporation of Carbide-derived carbon into polyamide membrane enhanced both CO_2 permeance (by 88.1 %) and CO_2/CH_4 selectivity (by 49.35 %) as a result of the higher free volume in the membrane matrix.
- The gas permeation of both CO_2 and CH_4 was found to increase with increasing the nanoparticles loading while CO_2/CH_4 selectivity improved up to 19.92 at 0.5% CDC loading then the selectivity deteriorated at 1% loading to 13.31.

- The effect of operating temperature on the separation performance was studied and the results showed improvements of gas permeation along with a decrease in CO_2/CH_4 selectivity as the temperature increased.
- By building more than one layer of polyamide on polysulfone support, gas permeance was found to decrease as a result of the increased resistance. The lower permeance was accompanied with a little increase in the gas selectivity.
- CO_2 permeance decreased with increasing the feed pressure. Whereas, CH_4 permeance increased which resulted in lower CO_2/CH_4 selectivity.

5.2 Recommendations:

The results and studies in this research work revealed that successful titanium carbide-derived carbon/polyamide membrane has been fabricated and showed potential enhancement in the separation performance. More studies, however, are needed to fully understand the characteristics of the polymer/nanofiller adhesion and the long term performance of the membranes. Regarding this issue the following recommendations can be advanced for future studies:

- Since natural gas is usually found at high pressure (up to 1000 psi) and temperature, it is recommended to test the CDC/Polyamide membranes at relatively high pressure to simulate the real process condition of the natural gas and to also study the plasticization of the membranes and it's effect on the separation performance.
- Titanium carbide-derived carbon showed potential to improve the separation performance of polyamide membrane so that CDC nanoparticles can be

functionalized by incorporating functional groups which have the ability to increase CO_2 permeability and thereby enhance CO_2/CH_4 selectivity.

References:

[1] Y. Zhang, J. Sunarso, S. Liu, R. Wang, International Journal of Greenhouse Gas Control Current status and development of membranes for CO_2 / CH_4 separation : A review,Int.J.Greenh.GasControl.12(2013)84–107. doi:10.1016/j.ijggc.2012.10.009.

[2] J.K. Adewole, A.L. Ahmad, S. Ismail, C.P. Leo, International Journal of Greenhouse Gas Control Current challenges in membrane separation of CO from natural gas : A review,Int.J.Greenh.GasControl. 17 (2013) 46–65. doi:10.1016/j.ijggc.2013.04.012.

[3] B. Shimekit, H. Mukhtar, Natural Gas Purification Technologies – Major Advances for CO_2 Separation and Future Directions, (n.d.).

[4] T.E. Rufford, S. Smart, G.C.Y. Watson, B.F. Graham, J. Boxall, J.C. Diniz, E.F. May, Journal of Petroleum Science and Engineering The removal of CO 2 and N 2 from natural gas : A review of conventional and emerging process technologies, J. Pet. Sci. Eng. 94-95 (2012) 123–154. doi:10.1016/j.petrol.2012.06.016.

[5] M.A. Aroon, A.F. Ismail, Performance studies of mixed matrix membranes for gas separation :Areview,Sep.Purif.Technol.75(2010)229–242. doi:10.1016/j.seppur.2010.08.023.

[6] T. Chung, L. Ying, Y. Li, S. Kulprathipanja, Mixed matrix membranes (MMMs) comprising organic polymers with dispersed inorganic fillers for gas separation, 32 (2007) 483–507. doi:10.1016/j.progpolymsci.2007.01.008.

[7] J. Albo, J. Wang, T. Tsuru, Application of interfacially polymerized polyamide composite membranes to isopropanol dehydration : Effect of membrane pre-

treatment and temperature, 453 (2014) 384–393.

[8] K.C. Wong, P.S. Goh, A.F. Ismail, Thin fi lm nanocomposite : the next generation selective membrane for CO_2 removal, J. Mater. Chem. A Mater. Energy Sustain. 4 (2016) 15726–15748. doi:10.1039/C6TA05145F.

[9] Y. Zhou, S. Yu, M. Liu, H. Chen, C. Gao, Effect of mixed crosslinking agents on performance of thin-film-composite membranes, 192 (2006) 182–189. doi:10.1016/j.desal.2005.05.029.

[10] S. Ver, K. Peinemann, J. Bordado, Thin-film composite hollow fiber membranes : An optimized manufacturing method, 264 (2005) 48–55.

[11] Y. Zhang, C. Xiao, E. Liu, Q. Du, X. Wang, Investigations on the structures and performances of a polypiperazine amide / polysulfone composite membrane, 191 (2006) 291–295. doi:10.1016/j.desal.2005.08.016.

[12] L. Lianchao, W. Baoguo, T. Huimin, C. Tianlu, X. Jiping, A novel nanofiltration membrane prepared with PAMAM and TMC by in situ interfacial polymerization on PEK-C ultrafiltration membrane, 269 (2006) 84–93.

[13] J. Zhao, Z. Wang, J. Wang, S. Wang, Influence of heat-treatment on CO 2 separation performance of novel fixed carrier composite membranes prepared by interfacial polymerization, 283 (2006) 346–356. doi:10.1016/j.memsci.2006.07.004.

[14] X. Yu, Z. Wang, Z. Wei, S. Yuan, J. Zhao, Novel tertiary amino containing thin film composite membranes prepared by interfacial polymerization for CO_2 capture, J. Memb. Sci. 362 (2010) 265–278. doi:10.1016/j.memsci.2010.06.043.

[15] S.S.Æ.B. Smitha, Æ.S. Mayor, B.P.Æ.T.M. Aminabhavi, Gas permeation properties of polyamide membrane prepared by interfacial polymerization, (2007) 9392–9401. doi:10.1007/s10853-007-1813-5.

[16] E.N. Hoffman, G. Yushin, B.G. Wendler, M.W. Barsoum, Y. Gogotsi, Carbide-derived carbon membrane, 112 (2008) 587–591.

[17] G. Dong, V. Chen, Challenges and opportunities for mixed-matrix membranes for gas separation, (2013) 4610–4630. doi:10.1039/c3ta00927k.

[18] A. Ebadi, M. Omidkhah, A. Kargari, The effects of aminosilane grafting on NaY zeolite – Matrimid s 5218 mixed matrix membranes for CO_2 / CH_4 separation, J. Memb. Sci. 490 (2015) 364–379. doi:10.1016/j.memsci.2015.04.070.

[19] S. Belhaj, A. Takagaki, T. Sugawara, R. Kikuchi, S.T. Oyama, Mixed matrix membranes using SAPO-34 / polyetherimide for carbon dioxide / methane separation, Sep. Purif. Technol. 148 (2015) 38–48.

[20] F. Dorosti, M. Omidkhah, R. Abedini, Journal of Natural Gas Science and Engineering Enhanced CO_2 / CH_4 separation properties of asymmetric mixed matrix membrane by incorporating nano-porous ZSM-5 and MIL-53 particles into Matrimid ® 5218, J. Nat. Gas Sci. Eng. 25 (2015) 88–102.

[21] H. Rabiee, S. Meshkat, M. Soltanieh, Journal of Industrial and Engineering Chemistry Gas permeation and sorption properties of mixed matrix membrane for CO_2 / CH_4 and CO_2 / N_2 separation, J. Ind. Eng. Chem. 27 (2015) 223–239. doi:10.1016/j.jiec.2014.12.039.

[22] M. Loloei, M. Omidkhah, A. Moghadassi, International Journal of Greenhouse Gas Control Preparation and characterization of Matrimid ® 5218 based binary and ternary mixed matrix membranes for CO_2 separation, Int. J. Greenh. Gas Control. 39 (2015) 225–235. doi:10.1016/j.ijggc.2015.04.016.

[23] M. Rezakazemi, A. Ebadi, Progress in Polymer Science State-of-the-art membrane based CO_2 separation using mixed matrix membranes (MMMs): An overview on current status and future directions, Prog. Polym. Sci. 39 (2014) 817–861. doi:10.1016/j.progpolymsci.2014.01.003.

[24] B. Zornoza, A. Martinez-joaristi, P. Serra-crespo, C. Tellez, ChemComm Functionalized flexible MOFs as fillers in mixed matrix membranes for highly selective separation of CO_2 from CH_4 at elevated pressures w, (2011) 9522–9524. doi:10.1039/c1cc13431k.

[25] B. Zornoza, C. Tellez, J. Coronas, J. Gascon, F. Kapteijn, Microporous and Mesoporous Materials Metal organic framework based mixed matrix membranes : An increasingly important field of research with a large application potential, Microporous Mesoporous Mater. 166 (2013) 67–78.

[26] M. Josephine, C. Ordo, K.J.B. Jr, J.P. Ferraris, I.H. Musselman, Molecular sieving realized with ZIF-8 / Matrimid ® mixed-matrix membranes, 361 (2010) 28–37. doi:10.1016/j.memsci.2010.06.017.

[27] E. Environ, T. Yang, T. Chung, Environmental Science Poly- / metal-benzimidazole nano-composite membranes for hydrogen, (2011) 4171–4180.

[28] Q. Song, S.K. Nataraj, M. V Roussenova, C. Tan, D.J. Hughes, W. Li, A. Alam, A.K. Cheetham, S.A. Al-muhtaseb, Supplementary information Zeolitic imidazolate framework (ZIF-8) based polymer nanocomposite membranes for gas separation, (2012).

[29] X. Li, L. Ma, H. Zhang, S. Wang, Z. Jiang, R. Guo, H. Wu, X. Cao, J. Yang, B. Wang, Synergistic effect of combining carbon nanotubes and graphene oxide in mixed matrix membranes for efficient CO_2 separation, 479 (2015) 1–10. doi:10.1016/j.memsci.2015.01.014.

[30] L. Ansaloni, Y. Zhao, B.T. Jung, K. Ramasubramanian, M. Giacinti, W.S.W. Ho, Facilitated transport membranes containing amino-functionalized multi-walled carbon nanotubes for high-pressure CO_2 separations, J. Memb. Sci. 490 (2015) 18–28. doi:10.1016/j.memsci.2015.03.097.

[31] F. Ranjbaran, M.R. Omidkhah, A.E. Amooghin, Journal of the Taiwan Institute of Chemical Engineers The novel Elvaloy4170 / functionalized multi-walled carbon nanotubes mixed matrix membranes : Fabrication , characterization and gas separation study, J. Taiwan Inst. Chem. Eng. 49 (2015) 220–228.

[32] R. Nasir, H. Mukhtar, Z. Man, M. Shima, Development and Performance Prediction of Polyethersulfone-Carbon Molecular Sieve Mixed Matrix Membrane for CO_2 / CH 4 Separation, 45 (2015) 1417–1422. doi:10.3303/CET1545237.

[33] A. Laeeq, S.P. Sree, J.A. Martens, M. Tayub, I.F.J. Vankelecom, Mixed matrix membranes comprising of matrimid and mesoporous COK-12 : Preparation and gas separation properties, J. Memb. Sci. 495 (2015) 471–478.

[34] S. Park, J. Bang, J. Choi, S. Hyup, J. Lee, J. Suk, 3-Dimensionally disordered mesoporous silica (DMS) -containing mixed matrix membranes for CO_2 and non-CO_2 greenhouse gas separations, Sep. Purif. Technol. 136 (2014) 286–295. doi:10.1016/j.seppur.2014.09.016.

[35] M. Waqas Anjum, F. de Clippel, J. Didden, A. Laeeq Khan, S. Couck, G. V. Baron, J.F.M. Denayer, B.F. Sels, I.F.J. Vankelecom, Polyimide mixed matrix membranes for CO_2 separations using carbon–silica nanocomposite fillers, J. Memb. Sci. 495 (2015) 121–129. doi:10.1016/j.memsci.2015.08.006.

[36] S.G. Lovineh, M. Asghari, G. Khanbabaei, CO_2 permeation through poly(amide-6-b-ethylene oxide)-nanosilica membranes, Appl. Surf. Sci. 318 (2014) 176–179. doi:10.1016/j.apsusc.2014.03.027.

[37] A. Ghadimi, T. Mohammadi, N. Kasiri, Gas permeation, sorption and diffusion through PEBA/SiO2 nanocomposite membranes (chemical surface modification of nanoparticles), Int. J. Hydrogen Energy. 40 (2015) 1–10.

[38] H. Adelnia, H. Cheraghi, A.F. Ismail, T. Matsuura, Gas permeability and permselectivity properties of ethylene vinyl acetate / sepiolite mixed matrix membranes, Sep. Purif. Technol. 146 (2015) 351–357.

[39] P.C. Oh, N.A. Mansur, Jurnal Teknologi Full paper Effects of Aluminosilicate Mineral Nano-Clay Fillers on Polysulfone Mixed Matrix Membrane for Carbon Dioxide Removal, 9 (2014) 23–27.

[40] M. Rezaei, A.F. Ismail, S.A. Hashemifard, G. Bakeri, T. Matsuura, International

Journal of Greenhouse Gas Control Experimental study on the performance and long-term stability of PVDF / montmorillonite hollow fiber mixed matrix membranes for CO_2 separation process, Int. J. Greenh. Gas Control. 26 (2014) 147–157. doi:10.1016/j.ijggc.2014.04.021.

[41] G. George, N. Bhoria, S. Alhallaq, A. Abdala, V. Mittal, Polymer Membranes for Acid Gas Removal from Natural Gas, (2015). doi:10.1016/j.seppur.2015.12.033.

[42] B. Chakrabarty, A.K. Ghoshal, M.K. Purkait, Preparation , characterization and performance studies of polysulfone membranes using PVP as an additive, 315 (2008) 36–47. doi:10.1016/j.memsci.2008.02.027.

[43] R.M. Boom, I.M. Wlenk, T. Van Den Boomgaard, C.A. Smolders, Microstructures in phase inversion membranes . Part 2 . The role of a polymeric additive *, 73 (1992) 277–292.

[44] Infrared and Raman Characteristic Group Frequencies Contents, n.d.

[45] E. Zera, W. Nickel, G.P. Hao, L. Vanzetti, S. Kaskel, G.D. Sorar, Nitrogen doped carbide derived carbon aerogels by chlorine etching of a SiCN aerogel, (2016) 4525–4533. doi:10.1039/C6TA00589F.

[46] K.W. Adu, Q. Li, S.C. Desai, A.N. Sidorov, G.U. Sumanasekera, A.D. Lueking, Morphological , Structural , and Chemical Effects in Response of Novel Carbide Derived Carbon Sensor to NH_3 , N_2O , and Air, (2009) 582–588.

[47] S.D. Bruck, Thermal Degradathgn of Piperazine Polyamides H Poly (terephthaloyl piperazine), Poly (terephthaloyl 2-meth- ylpiperazine) and Poly (isophthaloyl,

(n.d.) 231–241.

[48] C. Liang, P. Uchytil, R. Petrychkovych, Y. Lai, K. Friess, M. Sipek, M.M. Reddy, S. Suen, A comparison on gas separation between PES (polyethersulfone)/ MMT (Na-montmorillonite) and PES / TiO_2 mixed matrix membranes, Sep. Purif. Technol. 92 (2012) 57–63. doi:10.1016/j.seppur.2012.03.016.

[49] G.N. Yushin, E.N. Hoffman, A. Nikitin, H. Ye, M.W. Barsoum, Y. Gogotsi, Synthesis of nanoporous carbide-derived carbon by chlorination of titanium silicon carbide, 43 (2005) 2075–2082. doi:10.1016/j.carbon.2005.03.014.

[50] R. Dash, J. Chmiola, G. Laudisio, Titanium Carbide Derived Nanoporous Carbon for Energy-Related Applications Titanium Carbide Derived Nanoporous Carbon for Energy-Related, 44 (2006) 2489–2497.

[51] Y.A. Shepl, Y.H. Kotp, M.S. El-deab, H.A. Shawky, B.E. El-anadouli, Performance enhancement of TFC RO membrane by using magnesium silicate nanoparticles, (2012).

[52] K.C. Wong, P.S. Goh, B.C. Ng, A.F. Ismail, polymethyl methacrylate modi fi ed multi-walled, (2015) 31683–31690. doi:10.1039/C5RA00039D.

[53] E.O.H.D.B.A. Kostianoy, The Handbook of Environmental Chemistry, n.d.

[54] W.M. Mcdanel, M.G. Cowan, N.O. Chisholm, D.L. Gin, R.D. Noble, Fixed-site-carrier facilitated transport of carbon dioxide through ionic-liquid-based epoxy-amine ion gel membranes, J. Memb. Sci. 492 (2015) 303–311.

[55] S. Banerjee, G. Maier, C. Dannenberg, J. Spinger, Gas permeabilities of novel poly

(arylene ether) s with terphenyl unit in the main chain, 229 (2004) 63–71. doi:10.1016/j.memsci.2003.09.016.

[56] X. Li, I. Kresse, Z. Xu, Effect of temperature and pressure on gas transport in ethyl cellulose membrane, 42 (2001).

[57] S.K. Sen, S. Banerjee, Gas transport properties of fluorinated poly (ether imide) films containing phthalimidine moiety in the main chain, 350 (2010) 53–61. doi:10.1016/j.memsci.2009.12.011.

[58] S. Shahid, K. Nijmeijer, Performance and plasticization behavior of polymer – MOF membranes for gas separation at elevated pressures, J. Memb. Sci. 470 (2014) 166–177. doi:10.1016/j.memsci.2014.07.034.

VITAE

Name	Abdelrahman Mohammedelfatih Awad
Nationality	Sudanese
Date of Birth	09/04/1992
Email	abdalrahmanmohamed2050@hotmail.com abdalrahmanmohamed2050@gmail.com
Address	Dhahran, Eastern Province, Kingdom of Saudi Arabia
Academic Background	Bachelor of Science, Chemical Engineering (2008-2013) University of Khartoum, Sudan Master of Science, Chemical Engineering (2015-2017) King Fahd University of Petroleum and Minerals
Journal Publications	Abdelrahman M. Awad, Isam H. Aljundi, Interfacial polymerization of facilitated transport polyamide membrane prepared from PIP and IPC for gas separation applications (**under review)**
Conference papers	Conference Proceedings: Abdelrahman M. Awad, Isam H. Aljundi, Natural gas separation using Polysulfone membranes: optimization of evaporation time in dry/wet phase inversion method, Proceedings 4th Saudi International Nanotechnology Conference (SINC2016)., Dhahran Saudi Arabia, 25th -27th ,October 2016